

# FROM CRUST TO CORE AND BACK

EXPERIMENTAL GEOSCIENCES AT BAYERISCHES GEOINSTITUT

# FROM CRUST TO CORE AND BACK

EXPERIMENTAL GEOSCIENCES AT BAYERISCHES GEOINSTITUT



Universität Bayreuth  
95440 Bayreuth  
Germany

Tel. +49 (0) 921 - 553700

Fax +49 (0) 921 - 553769

email: [bayerisches.geoinstitut@uni-bayreuth.de](mailto:bayerisches.geoinstitut@uni-bayreuth.de)

homepage: [www.bgi.uni-bayreuth.de](http://www.bgi.uni-bayreuth.de)

Editor: Hans Keppler

Contributors: Andreas Audetat, Tiziana Boffa Ballaran, Audrey Bouvier, Leonid Dubrovinsky, Dan Frost, Gregor Golabek, Florian Heidelbach, Takaaki Kawazoe, Tomo Katsura, Catherine McCammon, Nobuyoshi Miyajima, Dave Rubie, Gerd Steinle-Neumann

Layout by: Petra Buchert

Printed by: Druckerei Schmidt & Buchta GmbH & Co. KG, Helmbrechts

All rights reserved. No part of this book may be reproduced or transmitted in any form or by any means, electronic or mechanical, including photocopy, recording or any information storage or retrieval system, without permission in writing from Bayerisches Geoinstitut.

© 2020 Bayerisches Geoinstitut – Universität Bayreuth, Bayreuth, Second Edition



The importance of Earth science has been widely recognised in recent years in the context of environmental change and global warming. While the current modifications in the Earth system are mostly due to human activity, in the geologic past climate change was caused by natural factors, such as volcanic activity or changes in solar irradiation. A quantitative understanding of what happened millions of years ago is essential for predicting the future of our planet, as these processes provide a natural experiment that illustrates the response of the Earth system to changing parameters. The continuous supply of raw materials – metals, minerals, or fossil fuels – for human technology is a prerequisite for human civilization. With the exhaustion of easily accessible deposits, it is becoming more and more difficult to meet global demand and only by a much-improved understanding of the formation conditions of deposits and better strategies for finding them has it been possible to sustain a growing human population. The shift to renewable energies will not change this situation fundamentally, it will only have the effect that other types of raw materials (*e.g.*, lithium for ion batteries) will move into the focus of economic interest. While natural disasters are rare in Germany, they are a major threat in other European countries, *e.g.*, in Italy where millions of people live near the volcanic centers of Vesuvius or the Campi Flegrei. However, the collapse of air traffic in nearly all of Europe after the eruption of Eyjafjallajökull in Iceland in 2010 illustrated nicely the vulnerability of modern societies to distant events – even from volcanoes that no one had ever heard of.

While we live on the surface of the Earth, understanding Earth's interior is essential for modelling the future of our planet, for

supplying essential raw materials to mankind and for mitigating natural hazards. Unfortunately, Earth's interior is not directly accessible for observation. Geophysical methods, *e.g.*, the observation of earthquake waves propagating through Earth's interior, can provide some insights into material properties deep in our planet. Translating these observations into models of composition and mineralogy, however, requires calibration by high-pressure and high-temperature experiments in the laboratory. Experimental data on material properties may be combined with geodynamic models that allow predicting the evolution of a planet through geologic time. Such models show, for example, that plate tectonics, as it exists on Earth is only possible in a rather narrow parameter space. Given the discovery of now more than 4000 exoplanets orbiting around distant stars, such models are of great interest, as they may predict how likely it is that Earth-like conditions and possibly life exist elsewhere in the universe.

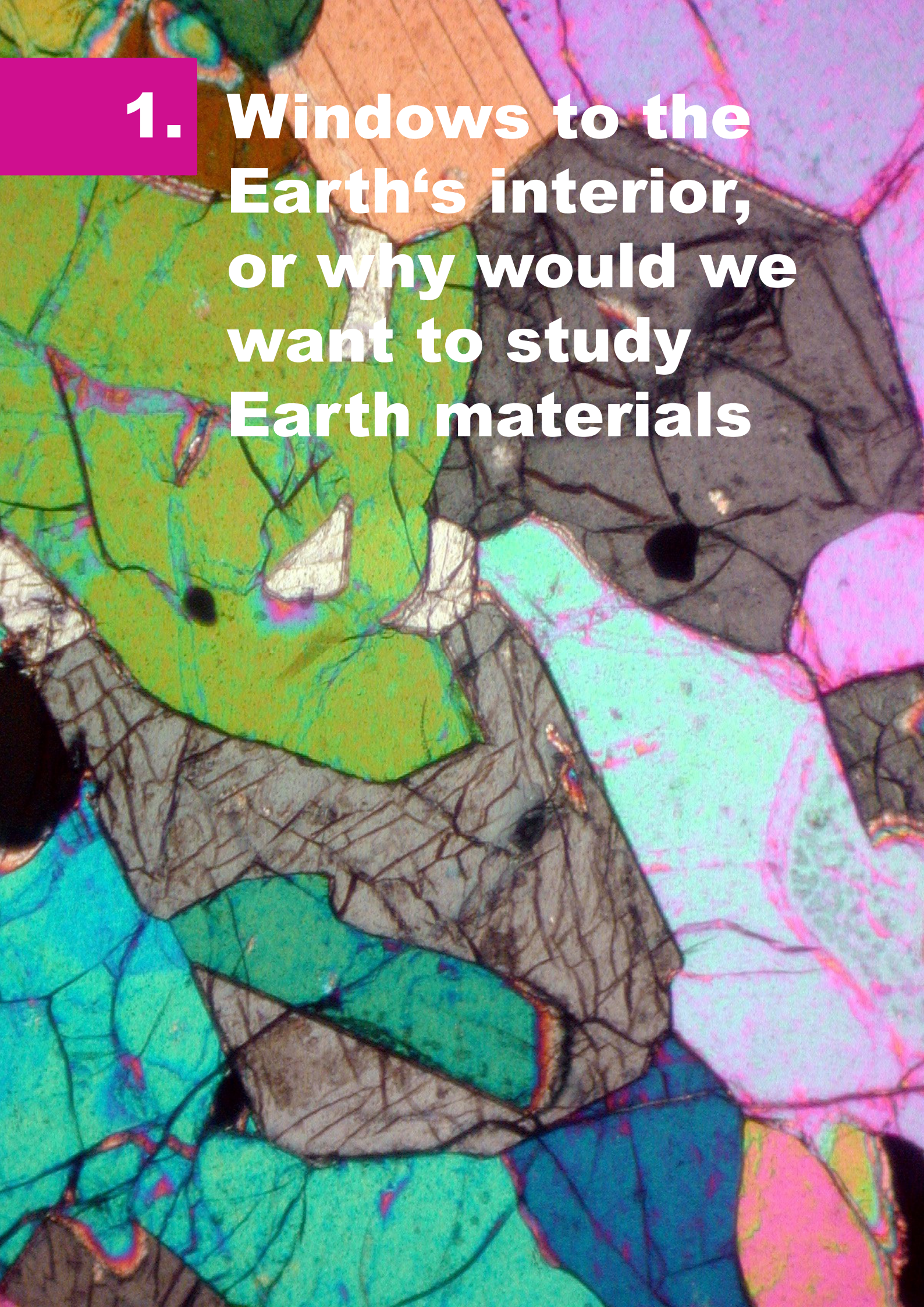
Bayerisches Geoinstitut was founded in 1986 by the State of Bavaria as a centre for high-pressure and high-temperature research in Earth sciences. Since then, it has evolved into one of the world's leading institutions in this field. For example, already a few years after the foundation of the institute, experiments in Bayreuth showed that ringwoodite, a high-pressure mineral stable in the transition zone of Earth's mantle at about 600 km depth, may be a major host of water in Earth's interior. In 2014, this was confirmed by the discovery of a ringwoodite grain containing about 1 wt. % of water in a natural diamond from the mantle. In this brochure, we provide an overview of the research at Bayerisches Geoinstitut, for scientists from other disciplines and also for the general public. We hope that you, the reader, will have much pleasure in browsing through this booklet.

Hans Keppler



## Table of Contents

1. Windows to the Earth's interior	6
2. The tools	14
3. A look to outer space: Meteorite and impact research	20
4. Early differentiation of the Earth	24
5. Mineral phase transformations and the structure of Earth's mantle	30
6. Volatiles in Earth's interior	34
7. The oxidation state of the Earth's interior	42
8. Mantle convection and rheology	46
9. The lower mantle	50
10. The Earth's core	54
11. Volcanism	58
12. Mineral resources	62
13. Technological applications	66
14. About Geoinstitut	70
Source of Figures	76



**1. Windows to the Earth's interior, or why would we want to study Earth materials**

The surface of the Earth on which we live is an interface, with interactions of endogenous (inner) and exogenous (outer) forces. For example, heat is supplied to us both by radiation from the sun, and by heat flux from the Earth's interior. Carbon dioxide released by volcanoes contributes to the greenhouse effect, while sulphate aerosols from explosive eruptions may backscatter sunlight. Both effects may lead to variations in surface temperature. Earthquakes originate from stress release in the Earth's brittle crust. Geochemical cycles may reach from the stratosphere down to the depths of the Earth's mantle, and auroras in the ionosphere are closely connected to the magnetic field originating from convection of liquid metal in the Earth's outer core. To understand the origin of all these phenomena, we have to investigate the processes – both present and past – that occur in the Earth.

Figure 1.1 shows our present understanding of the nature of the Earth's interior. The Earth may be described in an oversimplified "onion-shell" model as consisting of a thin crust (close to an average composition of granite on the continents and basalt under the oceans) with an ultrabasic

mantle (rock name peridotite) reaching down to about 2900 km depth. The mantle can be further subdivided on the basis of distinct mineral species into an upper mantle, a transition zone, and a lower mantle. The crust and the upper part of the upper mantle (to about 100 km depth) form the brittle "skin" of the Earth, called the lithosphere, which constitutes the rigid plates. These plates "swim" on the much more ductile (but still solid) rest of the mantle. Further down, the core extends from 2900 km to the Earth's centre at 6371 km depth. It consists mostly of iron, and is subdivided into a molten outer core and a solid inner core.

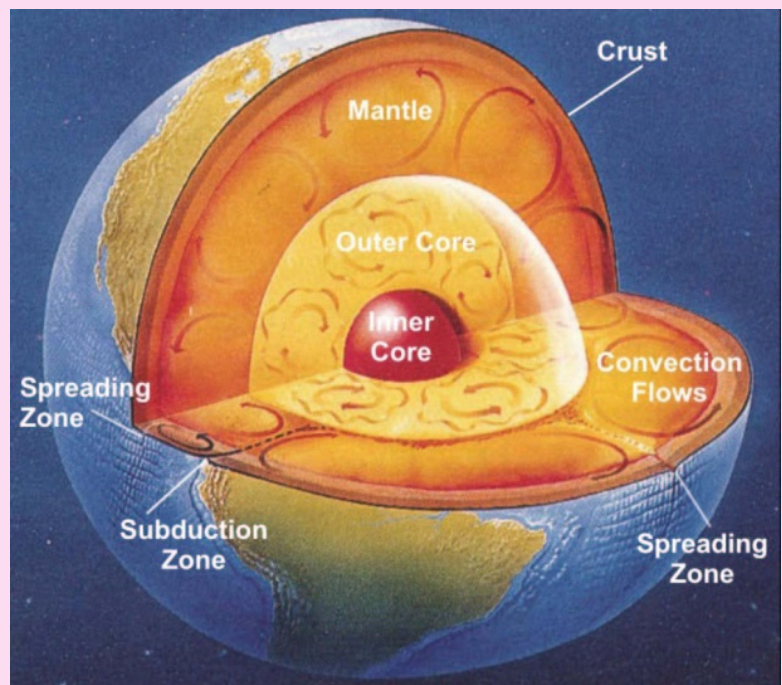


*Fig. 1.1: Schematic cross section through the Earth, showing the major units and several convection processes.*



*Fig. 1.2: Sample from the Earth's mantle enclosed within basalt. This greenish peridotite nodule, which consists of olivine, pyroxenes and spinel, was transported by the basaltic melt and then ejected. The length of nodule is ca. 12 cm.*

The Earth is a lively planet, and it is the dynamic nature of the processes that we feel as endogenous benefits or threats at the surface. Essentially, these dynamic processes are driven by a two-stage heat engine which derives its energy from the temperature gradient between the centre of the Earth and its surface. In the outer core, rapid convection in the liquid metal creates the dynamo which produces the Earth's magnetic field. In the mantle, the solid materials are at such high temperatures that they flow

plastically like toothpaste, where hotter and less dense materials rise slowly as diapirs, while colder and denser materials descend in the slabs at subduction zones.

How has the picture of the Earth presented in Figure 1.1 been derived? Mine shafts are at most a few kilometres deep and the deepest drillhole on Earth so far ended at 12 km depth. We therefore have to rely on a combination of more or less indirect but inter-linked approaches:

**Petrology and geochemistry:** Metamorphic rocks in mountain ranges may have formed at depths down to 100 km and then be uplifted again. Basaltic magmas form in the uppermost part of the Earth's mantle down to 60 km depth. On their way through the mantle, basalts often collect rock samples (xenoliths) and bring them to the surface (Fig. 1.2). Kimberlites are a rare type of magma with probably very explosive eruptions. They are very much sought after because they are the main source of diamonds on Earth. Although a kimberlite eruption has never been observed in historic time, it is well established that they originate in the mantle at 200 km depth or even deeper. While most diamonds formed within the uppermost part of the mantle, a small group appears to originate from greater depth, including some from below 670 km, which therefore represent samples of the Earth's lower mantle. The hard and resistant diamond may encapsulate mineral inclusions like a safe and protect them from chemical alteration during ascent (Fig. 1.3).

**Cosmochemistry:** According to the Kant-Laplace theory, the solar system originated as a rotating gas cloud, which upon cooling condensed partially to solid dust particles. The dust particles then collided to form small planetesimals and ultimately planets, including

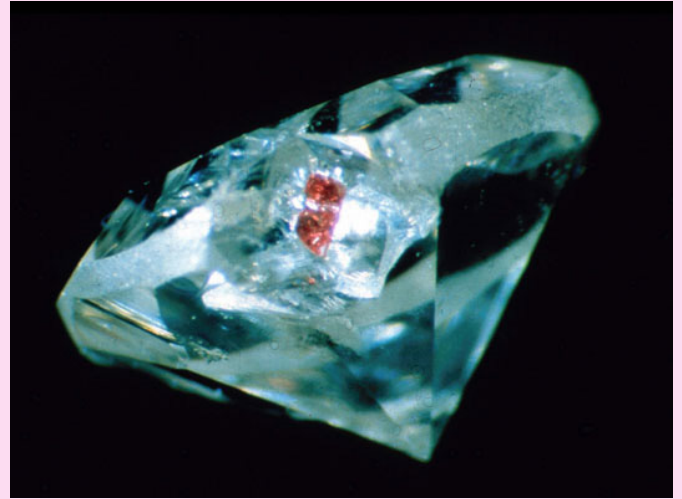


*Fig. 1.3: Bright red garnet inclusion in a round brilliant diamond.*

the Earth. Obviously, it would be very helpful if we had some samples of this material from which the Earth formed. These samples exist – they are so-called chondritic meteorites, which ultimately come from the asteroid belt between Mars and Jupiter. They are largely unchanged samples of the material from which the Earth formed more than 4.5 billion years ago (Fig. 1.4). These chondrites mainly consist of iron-nickel metal, silicate minerals, and sometimes carbonaceous material and minor sulphides. The relatively large mass and relatively small moment of inertia of the Earth, as derived from astronomical data, suggest that the material in the core should be much denser than that in the mantle and crust. Therefore, one may assume that Earth's core essentially was formed from the metal phase in the chondrites, while the silicates formed the mantle.

Allende meteorite



*Fig. 1.4: A piece of the Allende meteorite that fell in 1969 in Mexico. It is a carbonaceous chondrite; many of the small rounded grains are chondrules, solidified droplets of melts that formed in the early solar system. White grains are calcium-aluminium-rich inclusions (CAIs) formed by the condensation of nebular gas.*

**Geophysical observation:** Some physical properties of the deep Earth's interior can be estimated by geophysical methods. Seismology observes the propagation of mechanical waves from earthquakes through the body of the Earth. Subtle variations in seismic velocities can be used to construct three-dimensional tomographic images that reveal zones of warm upwellings or of cold slabs descending in the mantle (Fig. 1.5). The anisotropy of seismic wave velocities may be used to infer dynamical motion in the mantle. This is possible because the slow flow of mantle rocks over geologic time changes the orientation of mineral grains in them, such that the propagation of seismic waves

through these rocks becomes dependent on orientation. Magnetic fields in the ionosphere and magnetosphere of the Earth, produced by interactions with the solar wind, may induce electrical currents in Earth's interior, which in turn generate secondary electromagnetic fields that can be observed. They can be used to constrain the electrical conductivity in the mantle, which provides hints about the presence of volatiles and magmas that cannot be detected by seismology. Finally, the viscosity distribution in the mantle be estimated by precise observation of crustal motions, *e.g.*, the uplift of the Scandinavian shield after removal of the glaciers from the last ice age.

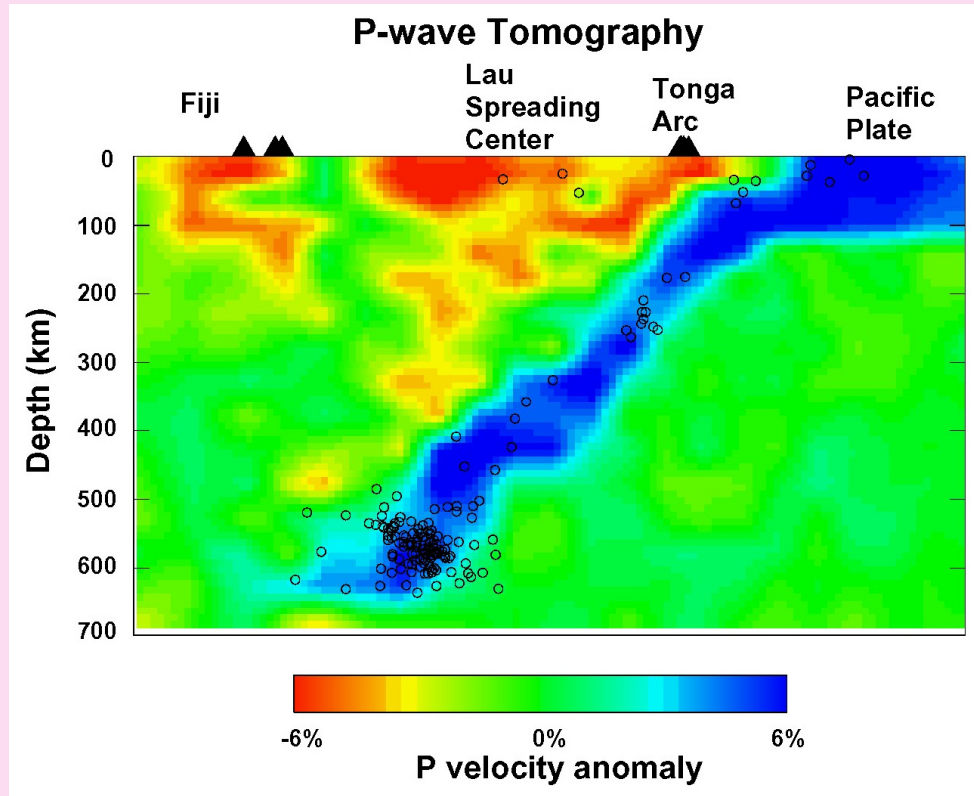


Fig. 1.5: East-west vertical cross section of seismic P-wave velocity to 700 km depth across the Tonga subduction zone and Lau Ridge. Red and blue colours denote slow and fast velocities. Solid triangles indicate active volcanoes, while earthquakes within 40 km width from the cross section are marked by circles.

**Geodynamic modelling:** Large scale geological processes such as subduction of oceanic crust or rising of mantle plumes may be successfully modelled in three dimensions using tools such as finite element methods. In this way, the distribution of physical parameters such as temperature, stress and buoyancy as well as the shape of chemical heterogeneities or the regions of stability or metastability of individual mineral structures can be predicted. Figure 1.6 shows the calculated temperature distribution in and around a cold subducted slab.

Such models require a detailed knowledge of material properties, such as thermal conductivity in this specific example.

Finally, there is **experimental geochemistry and geophysics**. This involves the laboratory determination of the properties of Earth materials under well-defined conditions of pressure, temperature and chemical composition, which is what most of this booklet is actually about. This approach can be considered a particular type of material

## Windows to the Earth's interior

science – the physics and chemistry and physical chemistry of matter, mostly specialised to extreme temperatures and pressures, and more or less confined to the chemical compositions that we expect in the Earth. Such laboratory data then provide constraints for the interpretation of observational data, for example the elastic properties derived from seismic wave velocities must conform to those of materials that are stable at the corresponding depths and chemical compositions. Laboratory data are also the basis for most modelling approaches, as exemplified by Figure 1.6. On the other hand, the output of the experimental approach depends on the

input (the chemical composition, for example), so ground truthing of experimental data by observations is therefore necessary.

In summary, we have to explore all relevant physical and chemical properties of Earth materials at the relevant conditions of pressure and temperature, as well as possibly others such as the fugacity of volatile species (water, for example). Pressure and temperature alone are a challenge: as shown in Figure 1.7 we have to cover a pressure range from *ca.* 0 to 365 GPa (1 Gigapascal = 10 000 times atmospheric pressure) and a temperature

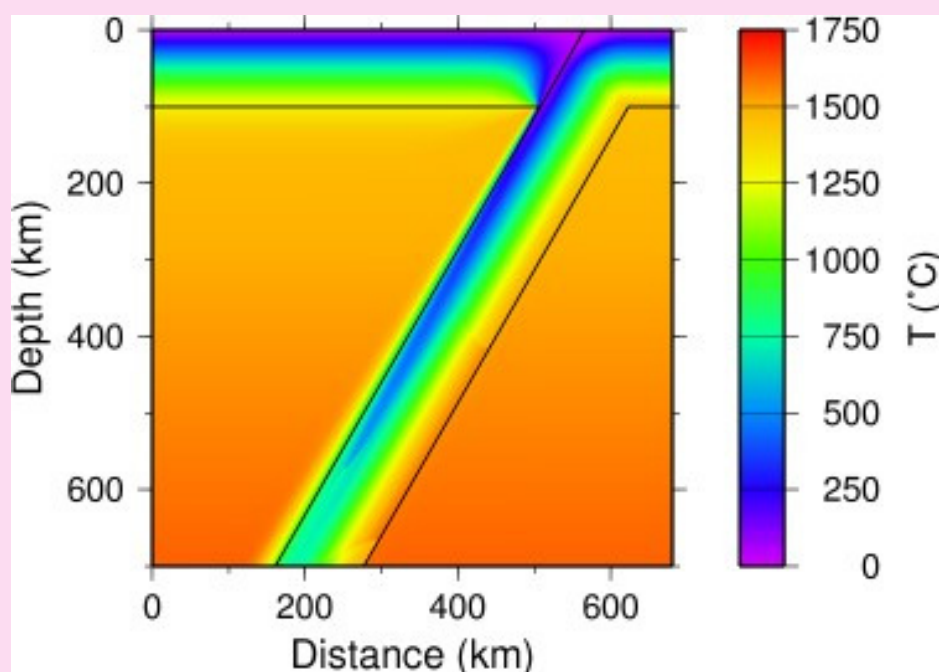


*Fig. 1.6: Calculated temperature distribution in a subducted slab. The cold subducted crust forms a wedge within hotter mantle material.*

range from *ca.* 0 °C to 5000 °C in order to straddle the conditions from the Earth's surface down to its centre. In

the next section, we will therefore look at the available methodology.

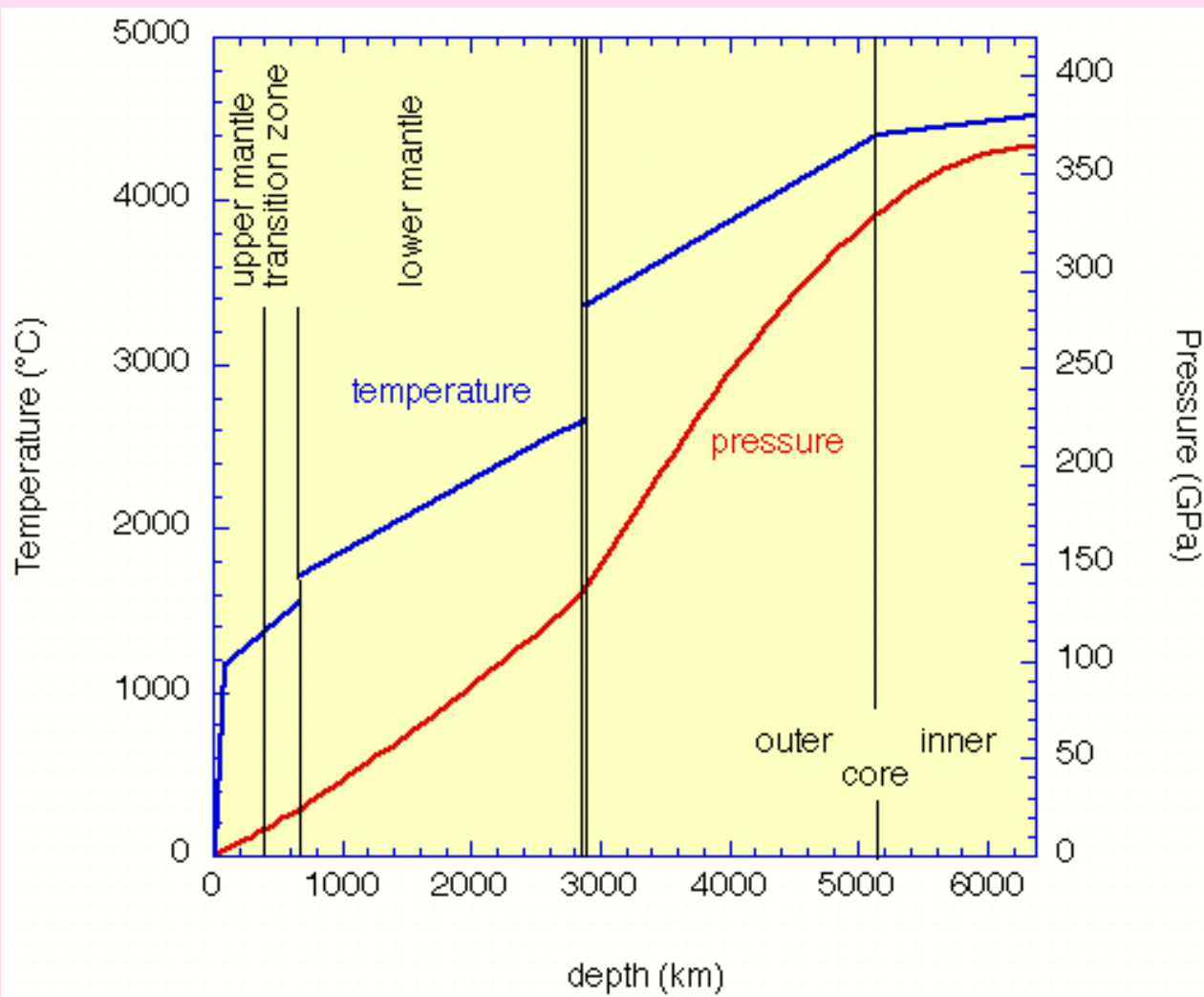


*Fig. 1.7: Pressure distribution in the Earth according to the Preliminary Reference Earth Model. The temperature estimate is uncertain, and at large depths the possible error is on the order of at least 1000 °C.*

## 2. The tools



To simulate the state of matter in the Earth's interior we may use a laboratory (or experimental *sensu stricto*) approach or computer modelling or – better still – a combination of both. The task is not trivial: as indicated in Figure 1.7, pressures cover the range from almost zero at the Earth's surface to 365 GPa at the centre of the core, temperatures vary from *ca.* 0 °C to *ca.* 5000 °C, materials include metals, oxides, sulphides, *etc.*, aggregate states range from solid to molten to fluid, crystal structures include both simple and complex ones, and bonding varies

from metallic to covalent to ionic. However, methodological development at Bayerisches Geoinstitut and elsewhere in the world has made it possible to tackle these tasks.

Pressure  $P$  is defined as  $P = F/A$

with  $F$  = force and  $A$  = area, and high pressures can be therefore generated in basically two ways: increasing the force or decreasing the area. The approaches are complementary, and both are used in Bayreuth.



Fig. 2.1: The multianvil laboratory at Bayerisches Geoinstitut showing (from right to left) the 1200, 1000 and 5000 ton presses.

## The tools

**Maximising force:** Bayerisches Geoinstitut operates seven large multianvil presses (with nominal capacities up to 5000 tons – Figure 2.1), which achieve pressures up to  $> 40$  GPa (corresponding to  $> 1200$  km depth) and temperatures up to  $3000$  °C, with "large" (up to several  $\text{mm}^3$ ) volumes. They operate by applying a large force (Fig. 2.2) to a sample assembly which incorporates a heater and a thermocouple for measuring temperature (Fig. 2.3). The anvils used to transfer the force to the



*Fig. 2.2: The 1000 ton multianvil press, opened for loading a sample assembly. The lower guide block (centre) contains the set of three outer anvils and the cubic arrangement of eight inner anvils (cf. Fig. 2.3), electrically insulated by green epoxy sheets.*

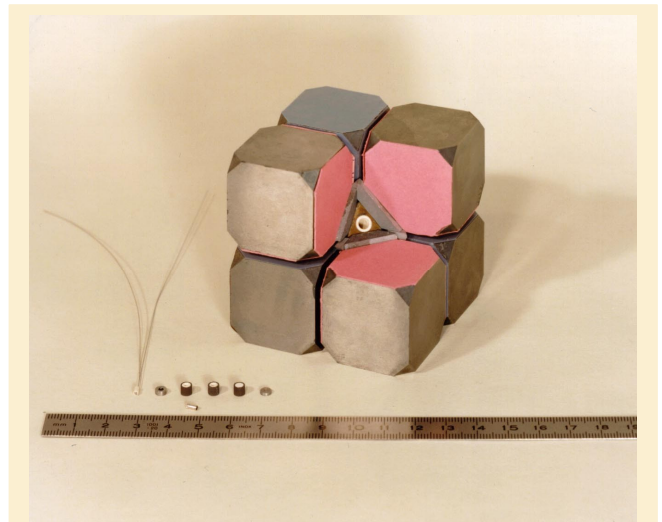


*Fig. 2.3: The set of eight inner tungsten carbide anvils, with one cube removed to show the ceramic octahedron serving as a pressure-transmitting medium. The thermocouple and the ceramic parts forming the furnace are shown on the lower left of the cube assembly.*

sample are made either of tungsten carbide (up to 25 GPa) or of sintered diamond (for up to 40 GPa and beyond). A typical feature of traditional multianvil technology is the use of a guideblock (Fig. 2.2), which redirects the force from a single hydraulic ram such that a confining force acting from several directions onto the sample is generated. In contrast to this, a new press developed at Bayerisches Geoinstitut (Fig. 2.4) uses six independently controlled rams to transfer pressure to the sample. This kind of press therefore allows controlled deformation experiments for simulating the flow of Earth's mantle in the laboratory. The press is also useful for containing quite large samples under high



Fig. 2.4: The new six-axes press developed at Bayerisches Geoinstitut. Six independently controlled hydraulic rams (800 tons each) can be used for deformation experiments under mantle conditions or for working with large sample volumes, e.g., in neutron diffraction experiments.

pressure and for this purpose, it is used at the SAPHiR facility of Bayerisches Geoinstitut at the FRM II neutron source in Garching for *in situ* neutron diffraction experiments.

**Minimising area:** In diamond anvil cells (DACs) two anvils made from superhard materials squeeze a tiny (10-500  $\mu\text{m}$ ) sample (Fig. 2.5); hence the required forces are relatively moderate. In this way pressures up to several hundred GPa may be attained. Heating may be external (up to about 1200  $^{\circ}\text{C}$ ) or internal using a laser. With 1000 GPa or 1 Tera-pascal, scientists at Bayerisches Geoinstitut achieved the highest pressure

ever obtained in a diamond cell, about three times the pressure in the centre of the Earth. DACs have the great advantage that the anvils are transparent to a wide range of electromagnetic radiation (X-rays, visible and infrared radiation, *etc.*) and samples can therefore be monitored during the experiments.

Some high-pressure materials may be brought back to room pressure without loss of structure or change in chemistry and can be studied at ambient conditions using a wide spectrum of methods such as electron microscopy, diffraction of X-rays or

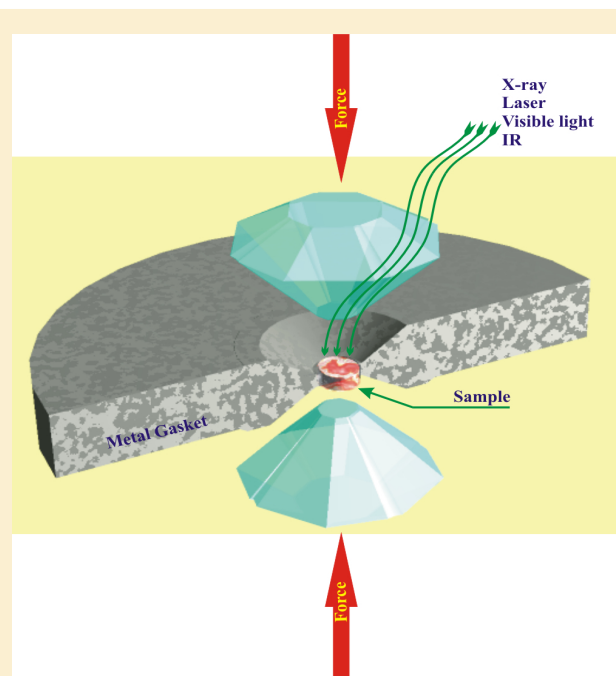
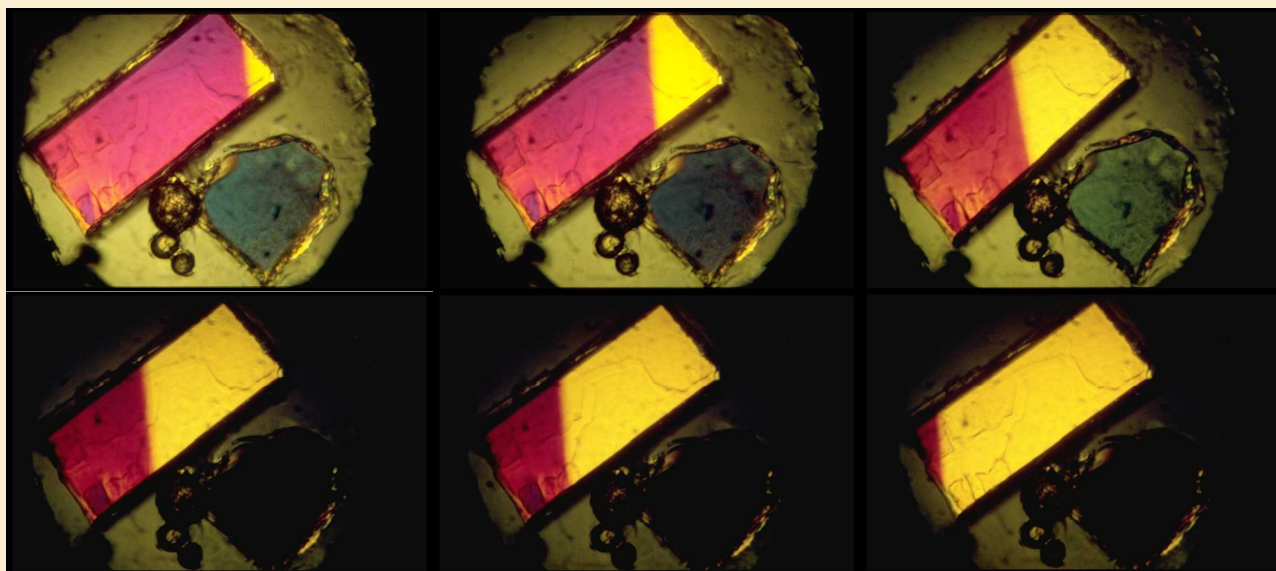


Fig. 2.5: Schematic cross section through a diamond anvil cell. The tiny sample is compressed between the diamond anvils, and heated and observed with the aid of electromagnetic radiation.

## The tools

neutrons or electrons, and various types of spectroscopy (see equipment list in the Appendix). In contrast, however, other materials decompose during decompression or change to a different structural state, and therefore require characterisation at high pressure and/or temperature by so-called *in situ* measurements (Fig. 2.6). Also, some critical properties of materials, such as compressibility or thermal conductivity, can only be studied at elevated pressures and temperatures. Work at Bayerisches Geoinstitut has solved some of these methodological challenges, and specific examples are given in the following sections.

**Computational methods** increasingly supplement experimental efforts in mineral physics. The electronic structure that is responsible for bonding is usually described with density functional theory (DFT), in which the electronic charge density (Fig. 2.7) serves as the basic property. Within the electronic structure calculations forces and stresses are computed and can be used to perform high temperature simulations through molecular or lattice dynamics. Such computations are free from experimental input and rely solely on chemical composition, the crystallographic structure and associated cell volume. By compress-



*Fig. 2.6: In situ observation of a phase transition in the diamond anvil cell as seen in a microscope between crossed polarisers. The spodumene crystal (a pyroxene of composition  $\text{LiAlSi}_2\text{O}_6$ ) transforms from a low-pressure (yellow) to a high-pressure (violet) form. A slight volume decrease at 3.2 GPa sweeps the interface (corresponding to the locus of the phase transition) between the two structures through the crystal. The high-pressure structure cannot be quenched, so measurements such as X-ray structure determination can only be made in situ at high pressure.*

ing the cell volume high pressure can be accessed easily.

Often, simulations are used to compute physical properties that are difficult to measure, to explore physical properties at conditions that are difficult to access in experiments, or to investigate the underlying physical causes for a particular phenomenon. All thermodynamic properties (in-

cluding elasticity, specific heat, and thermal expansivity) can be obtained from such simulations. Methodological developments and advances in computer technology now allow the computation of transport properties for which large simulation cells and long run durations are required at the DFT level, such as diffusivity in liquids and electronic and thermal conductivity of metals.

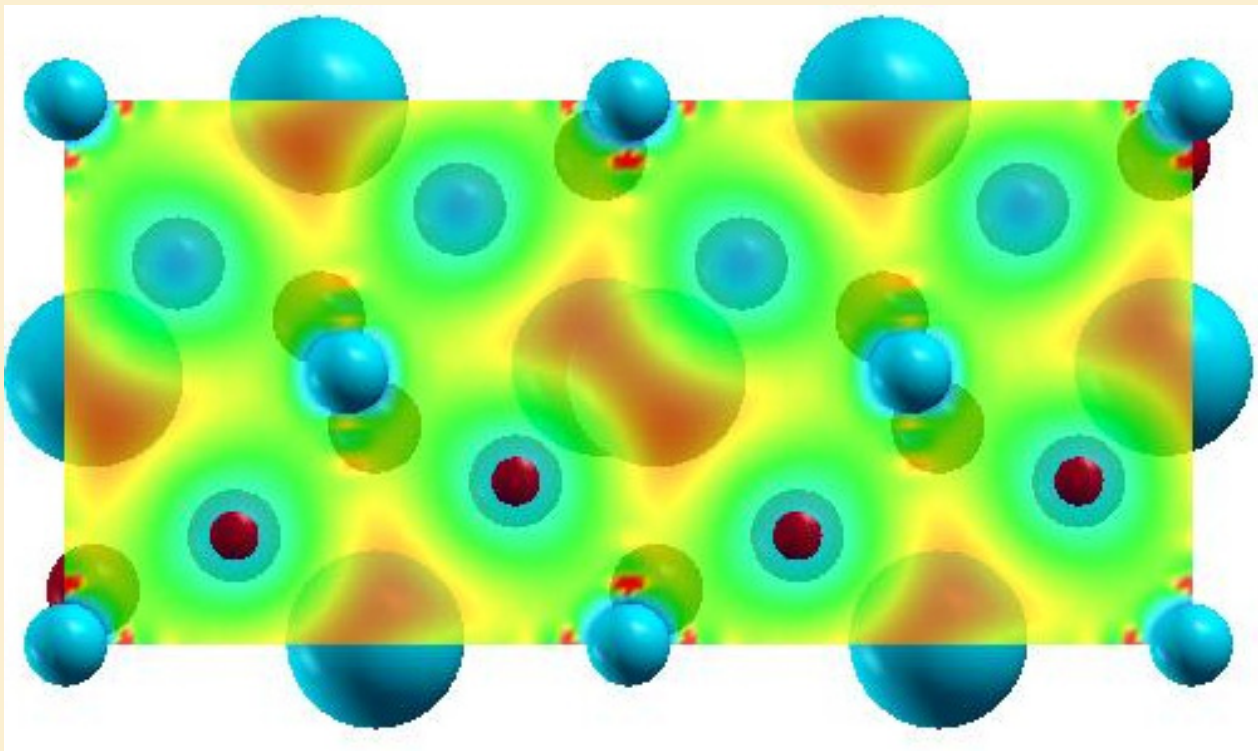


*Fig. 2.7: Calculated charge density of  $\text{MgSiO}_3$  perovskite shown for the  $a$ - $c$  plane. The structure is depicted as follows: Mg atoms (large blue spheres), Si atoms (small blue spheres) and O atoms (red spheres). The octahedral tilt of  $\text{SiO}_6$  octahedra in the orthorhombic  $Pbnm$  structure is apparent by two O atoms above the  $a$ - $c$  plane, and two O atoms below the plane. The charge density in the plane is displayed on a logarithmic scale: high charge density is dark brown and low charge density is red.*



# **3. A look to outer space: Meteorite and impact research**

Meteorites are the oldest materials of our solar system and supply information on its early history, which started about 4.6 billion years ago with the gravitational collapse of a cloud of interstellar gas and dust. Chondritic meteorites, in particular, represent the most primitive solar system materials. They consist mainly of chondrules, Fe-Ni metal, refractory calcium-aluminum-rich inclusions (CAIs), amoeboid olivine aggregates and fine-grained matrix material. All these components have been formed as independent objects in the solar nebula by high-temperature processes that included condensation and evaporation in a very inhomogeneous environment. Moreover, they have experienced multiple episodes of melting, impact-induced shock and secondary mineralisation during accretion in the nebula and in asteroid parent bodies. The mineralogy, chemistry and isotopic composition of primitive meteorites and their components may reveal fundamental details of their formation and evolution in the early Solar system. However, only results from well constrained experiments can lead to a correct interpretation of natural observations.

One of the open questions we want to address with our current research concerns the chemical and physical conditions at which the first solid materials

formed in the solar nebula. Among the chondritic components, CAIs have been extensively investigated in order to clarify temperature and oxygen fugacity conditions of the solar nebula because they yield the oldest measured ages of any solar system material. Measurements of the oxidation state of titanium in clinopyroxenes, spinel and hibonites, for instance, have been used to constrain the oxygen fugacity of the early solar nebula. Such measurements, however, rely on well calibrated oxybarometers, which can be determined only experimentally using synthetic samples obtained at known oxygen fugacity and temperature conditions and accurately characterised in terms of chemistry and cation distribution (Fig. 3.1).

Meteorites also give us direct access to natural samples of high-pressure silicates (*e.g.*, ringwoodite, majorite, bridgmanite, seifertite) which are believed to exist in the Earth's deep mantle. These high-pressure minerals occur in shock-melt veins resulting from asteroid impacts in space. High-pressure and high-temperature conditions are generated during such collisions and the local concentration of stress may cause transformations to high-pressure polymorphs in and close to melt veins. The characterisation of such shock-melt veins provides crucial information on the collision history of the parent bodies of

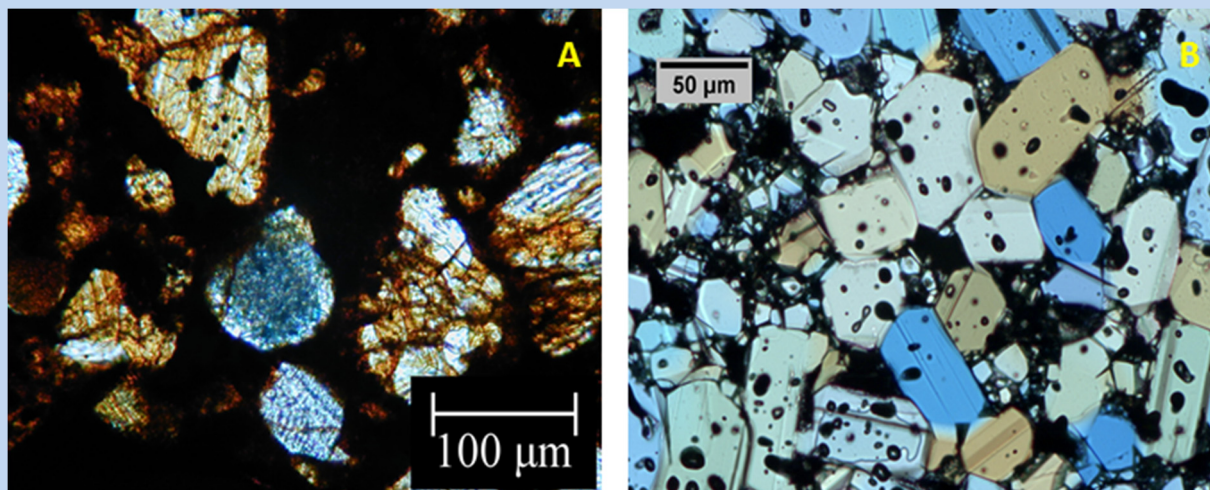


*Fig. 3.1: A) Plane-polarised transmitted light image of a thin section of the carbonaceous chondrite Acfer 182. The blue round object at the centre of the image is a typical calcium-aluminium-rich inclusion (CAI) containing grossite, hibonite, melilite and perovskite. The blue color is due to the presence of hibonite which contains titanium in different oxidation states. B) Plane-polarised transmitted light image of large single crystals of Ti-Mg-bearing hibonite synthesised at 1500 °C under reducing conditions. Hibonite coexists with Ca-Ti-perovskite (small light grains), similar to what has been observed in CAIs. The blue colour and the spectroscopic properties of these crystals are identical to those of the meteoritic sample. The use of large single-crystals allows a determination of the crystal-chemical properties of this mineral and hence an interpretation of the spectroscopic data of natural samples.*

these meteorites. Certain groups of meteorites, like the L6 chondrites and the Martian shergottite achondrites, have recorded very large shock pressures and temperatures (Fig. 3.2). Such conditions can, however, only accurately be determined by comparison with results from high-pressure/high-temperature experiments aimed to constrain the transformation mechanisms and element partitioning of silicate phases.

The presence and speciation of volatiles in planetary magmas is critical for controlling eruption dynamics. On Earth, volatiles are continuously cycled

between crust and mantle through plate tectonics, whereas lunar basalts have never come in contact with liquid water, as evidenced by the pristine olivine phenocrysts found in samples returned by the Apollo missions (Fig. 3.3). The only objects in the solar system, other than Earth, to show evidence of recent tectonic activity and volcanism are some planets and satellites in the outer solar system (Fig. 3.4). Since these planetary bodies are mainly comprised of icy compounds of water, ammonia and methane, information on the viscosity of ices under planetary interior conditions is required to model their accretion,

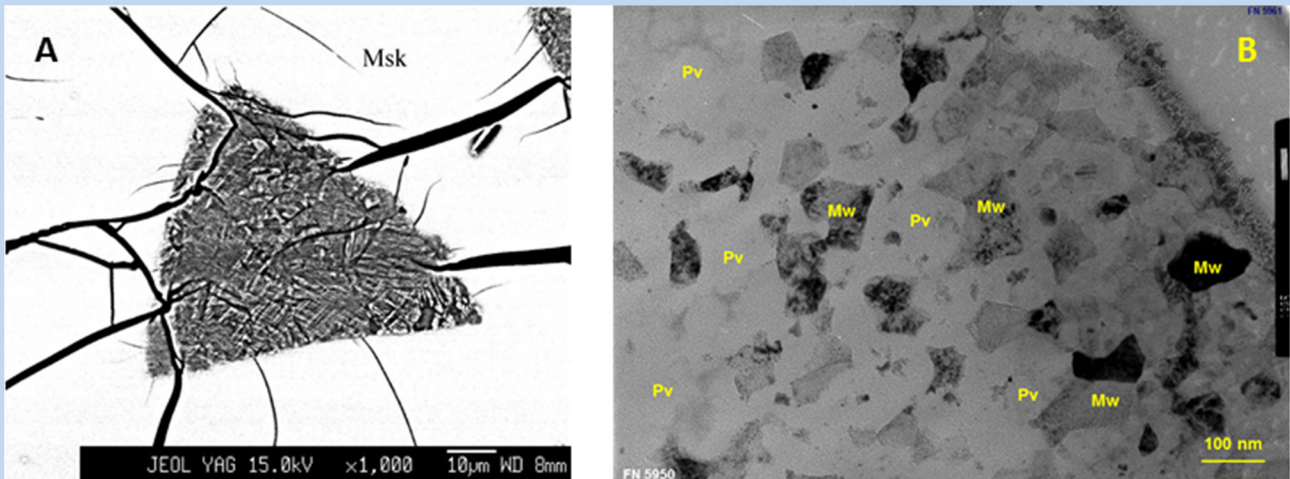


Fig. 3.2: A) Backscattered electron (BSE) micrograph of a triangular dense silica grain from the Shergotty meteorite originating from Mars. The large silica grain shows the typical pre-shock morphology and habit of tridymite or cristobalite and consists of numerous domains. Each domain displays an orthogonal pattern of bright (seifertite) and dark (dense SiO<sub>2</sub> glass) lamellae. B) TEM image of the dissociation of an olivine phenocryst adjacent to a shock melt vein of DaG 735 shergottite into (Mg,Fe)SiO<sub>3</sub> silicate perovskite (Pv), now called bridgmanite and magnesiowustite (Mw).

evolution and dynamic processes, just as the rheology of silicate materials is crucial to the understanding of Earth's convective processes. Viscosities of icy materials can only be obtained through the experimental study of rheological

and mechanical properties such as those currently undertaken at Bayerisches Geoinstitut.

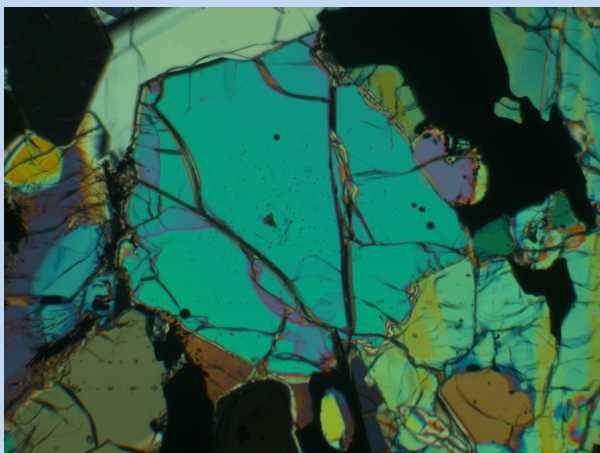


Fig. 3.3: Olivine phenocryst in lunar basalt 12005, Apollo 12.

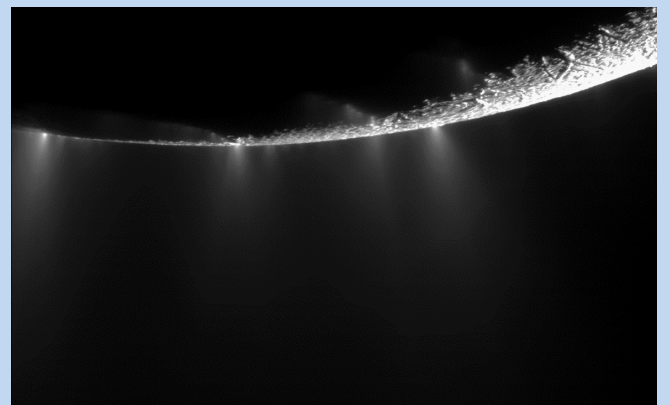


Fig. 3.4: Dramatic plumes, both large and small, spray water ice and vapour from many locations along the famed "tiger stripes" near the south pole of Saturn's moon Enceladus. The tiger stripes are four prominent, approximately 135 km long fractures that cross the moon's south polar terrain.

# 4. Early differentiation of the Earth



The Earth formed about 4.6 billion years ago through collisions with smaller planetary bodies that included large numbers of kilometre- to multi-kilometre-size planetesimals and a smaller number of Moon- to Mars-size embryos. These bodies formed from material that condensed in the solar nebula, some of which is represented today by chondritic meteorites. The fact that the Earth's interior consists today of chemically distinct regions – the metallic iron-rich core and the silicate mantle – indicates that a major differentiation event occurred during the early history of the Earth. This event caused metal to segregate from silicate and, because of its relatively high density, to sink to the Earth's central region to form the core (Fig. 4.1). For this process to be physically possible, the metal, and possibly also the silicate, must have been in a molten state. The heat that caused melting was produced by the decay of short-lived radioactive isotopes (*e.g.*,  $^{26}\text{Al}$ ) during the first 2-3 million years of solar system history and later by highly-energetic collisions between planetary bodies (Fig. 4.2). The mechanisms by which metal can segregate from silicate depend on whether or not the silicate is molten or crystalline and constraining them is therefore important for understanding the early thermal history of the Earth. For example, the giant impact theory, according to which the Earth

collided with a Mars-size embryo during the late stages of accretion (Fig. 4.2), resulting in the formation of the Moon, can be tested. The enormous energy involved in such collisions would have partially or wholly melted the Earth, leading to the formation of a deep magma ocean (Fig. 4.1).

A record of the process of core formation is preserved in the geochemistry of the Earth's silicate mantle. It is well known that siderophile ("metal-loving") elements, such as Fe, Ni, Co, W, Mo, and Pt partition strongly into metal, so that the concentrations of these elements in co-existing silicates is low. Indeed, the Earth's mantle is depleted in such elements as a consequence of metal-silicate equilibration and subsequent metal segregation during core formation. As the degree of depletion of each element is, in general, controlled by temperature, pressure and oxygen fugacity, experimental studies of the metal-silicate partitioning of siderophile elements are performed in order to understand the conditions of core formation. Early partitioning studies, performed at atmospheric pressure (1 bar) and moderate temperatures, suggested that siderophile element depletion in the mantle is much less than expected, so that the concentrations of such elements in the mantle appeared to be too high, often by orders of magnitude. The explanation

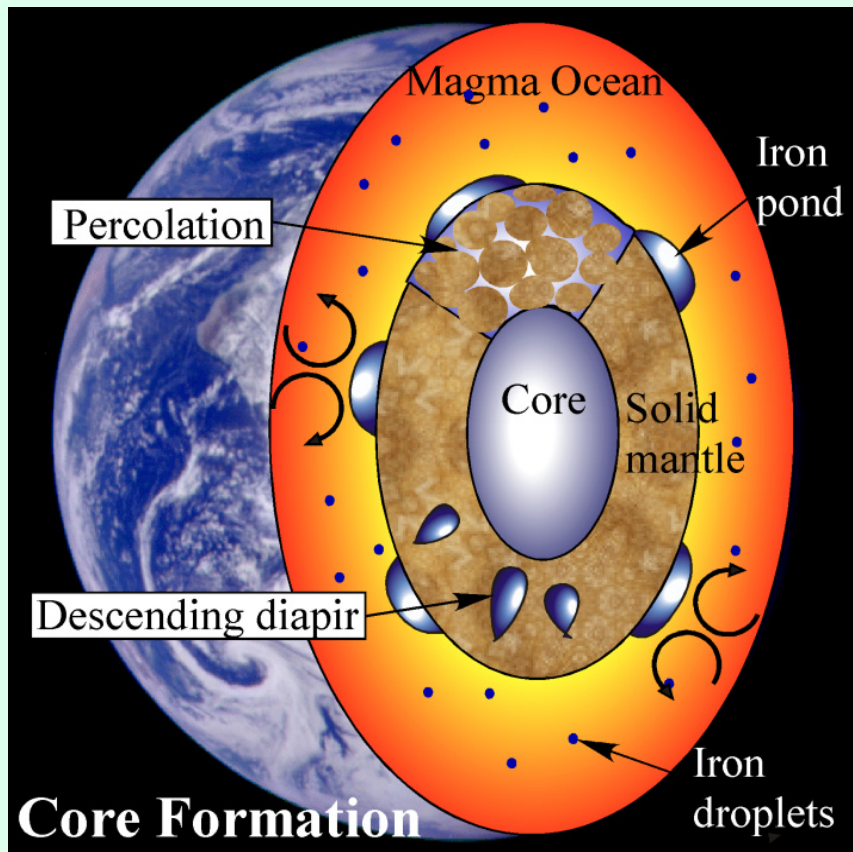


*Fig. 4.1: Schematic view of the Earth's interior during core formation illustrating the possible mechanisms by which liquid metal can segregate from crystalline or liquid silicates. A deep convecting magma ocean enables the iron cores of impacting bodies, possibly dispersed as small droplets, to sink and segregate efficiently and to accumulate as "ponds" above the crystalline lower mantle. The ponded metal descends further towards the proto-core either as km-size diapirs (with little chemical interaction) or by grain scale percolation through the crystalline silicates.*

for this apparent anomaly became apparent in the 1990s when it was discovered – among others, by work at Bayerisches Geoinstitut – that high pressures and temperatures have a strong effect on the partitioning of these elements. Thus, over the past years, numerous experimental studies have been performed to study the effects of pressure, temperature and oxygen fugacity on the partitioning of siderophile elements between metal, silicates and oxides up to

25 GPa and 3000 K using the multianvil apparatus (Fig. 4.3a). Results suggest that mantle concentrations of siderophile elements can be explained by core-mantle equilibration at pressures as high as 50 GPa and temperatures of 3500-4000 K. At these conditions, both metal and silicate would be in a molten state and the results are therefore consistent with metal-silicate segregation occurring in a magma ocean at a depth as great as 1400 km. However, there are



*Fig. 4.2: Artist's portrayal of a giant impact between two planetary bodies. At typical impact velocities of around 10 km/s, the inevitable consequence is large-scale melting and magma ocean formation.*

two problems with this result. First, experimental data obtained up to 25 GPa and 3000 K have to be extrapolated to much higher pressures and temperatures, which results in significant uncertainties. Second, single-stage core formation, involving materials of the mantle and core equilibrating at a single pressure-temperature condition, is physically unrealistic.

In order to reduce uncertainties in extrapolating experimental data from the

multianvil press to higher pressures and temperatures, laser-heated diamond anvil cells (LH-DAC) are now being used to investigate the partitioning of siderophile elements between liquid metal and silicate up to 100 GPa and 5000 K. Performing such experiments is challenging, especially because of high temperature gradients and the need for rigorous temperature measurements. In addition, analysing the resulting samples is difficult because of the very small size of the samples (Fig. 4.3b). Samples

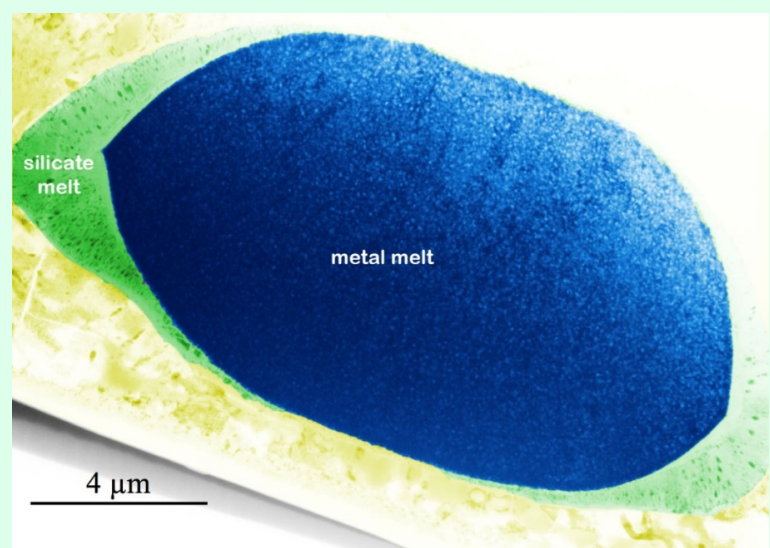
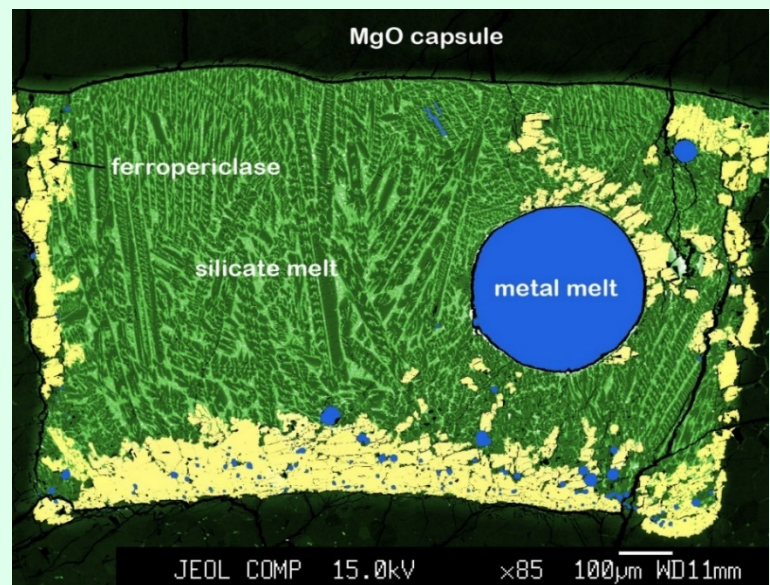
## Early differentiation of the Earth

are sectioned first by using the focused ion beam (FIB) technique. Analysis then requires the use of analytical transmission electron microscopy and sometimes nano-SIMS when element concentrations are very low.

Planetary accretion involves numerous collisions with smaller bodies, each of which delivers energy to the accreting planet (causing melting) and iron-rich metal which segregates to form the

core. Thus, core formation in the terrestrial planets (Mercury, Venus, Earth and Mars) was a complex multistage process involving many episodes of metal-silicate equilibration over a range of temperatures and pressures and a time scale up to 100 million years or more. More realistic multidisciplinary models of planetary evolution are now being developed by combining astrophysical "N-body" simulations of planetary accretion with core-mantle differentiation

*Fig. 4.3: Samples produced in a multianvil experiment (a) and a diamond anvil cell experiment (b), at 11 GPa/2473 K and 100 GPa/5500 K, respectively. By analysing the compositions of the co-existing quenched silicate and metal melts, the partitioning of siderophile elements between these phases can be determined as a function of pressure and temperature and then applied in models of core formation. Note the small size of the diamond cell sample. The images were produced by an electron microprobe and are colour-coded according to chemical composition.*



models. The latter are based on a rigorous mass balance approach that also enables the concentrations of light elements (Si, O, S and H) in planetary cores to be estimated. The constraints on such combined models include the masses and orbital characteristics of the terrestrial planets, the compositions of the mantles of Earth, Mars, Mercury and possibly Venus, and the mass fractions of the cores of these planets. Such combined models now enable the bulk compositions of primitive solar system bodies to be estimated as a function of their heliocentric distances of origin. These models place strong constraints on the accretion of water to the Earth and the other planets. In the future, core formation models can be further developed by also calculating the depth of melting associated with each impact event in the N-body accretion simulations.

Earth appears isotopically most alike to enstatite chondrites, but not elementally. Compared to the different groups of known chondrites, the Earth shows the strongest depletion in moderately to highly volatile elements. It is still a puzzle whether this difference is a consequence of unknown planetary materials forming the Earth or of fractionation processes during accretion.

A recently developed numerical approach for studying the early evolution of terrestrial planets is the coupling of SPH (smoothed particle hydrodynamics) collision results with three-dimensional high-resolution geodynamical models. Such models may simulate core formation and the generation of early crust on accreting planetary embryos (Fig. 4.4).

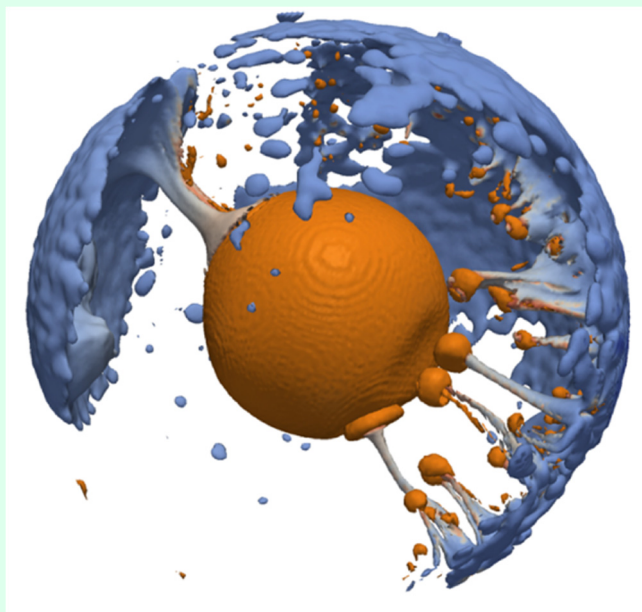
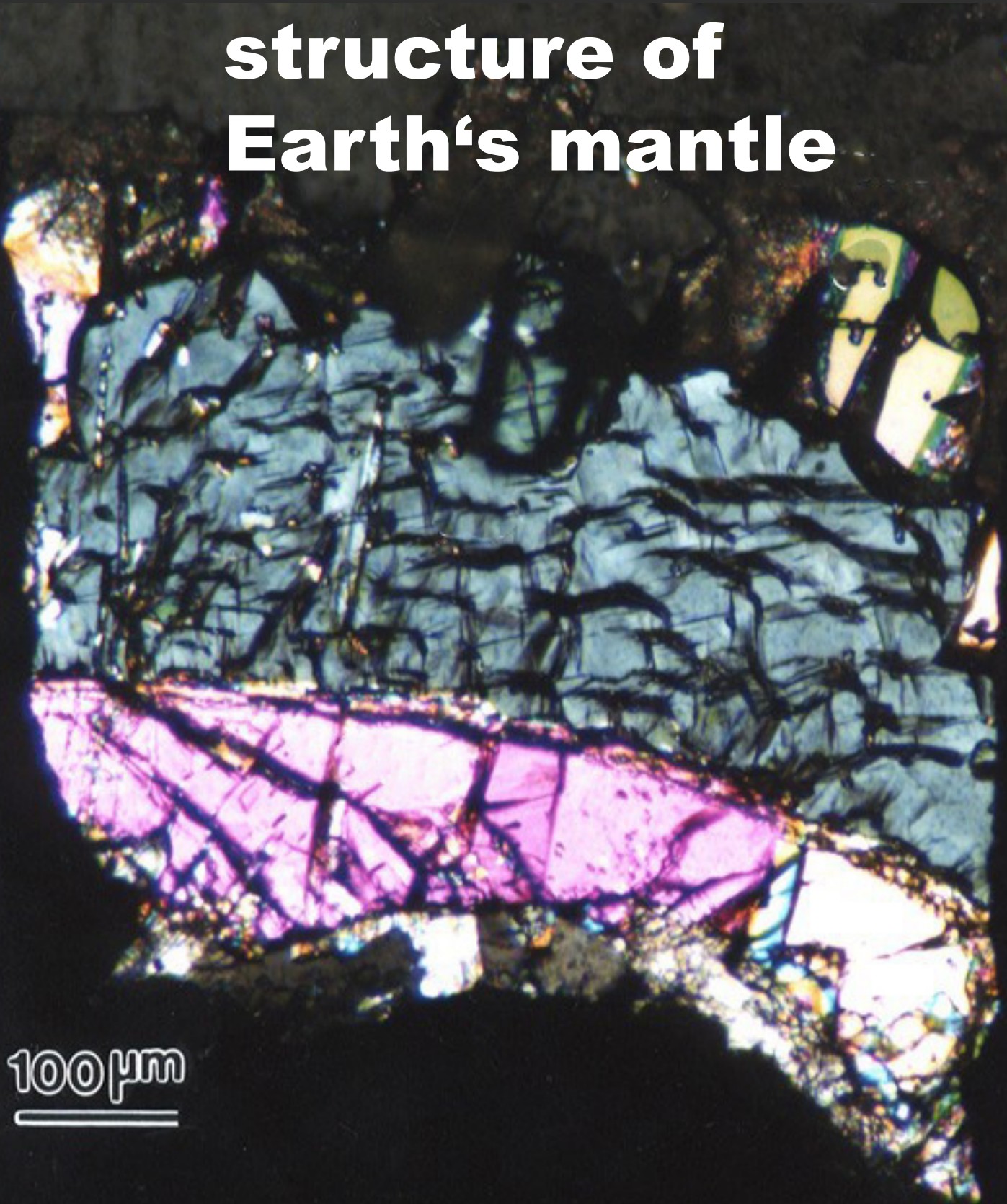


*Fig. 4.4: Numerical modelling of core formation (brown) and magma ocean crystallisation (dark and light blue) on a Mars-sized planetary embryo shortly after a grazing giant impact.*

# 5. Mineral phase transformations and the structure of Earth's mantle



100 μm

Rock samples from the mantle, brought to the surface in volcanic eruptions, mainly originate from depths of less than 200 km. What the remaining 2700 km of unsampled mantle is made of is, therefore, a very important question. The best evidence for the nature of the deeper mantle comes from seismology. Models developed from seismic wave travel times through the Earth indicate that the seismic wave velocities and density increase with depth both smoothly and discontinuously as shown in Figure 5.1. There are two major discontinuities at approximately 410 and 660 km depth that are caused by jumps in mantle density of around 4 % and 9 %, respectively. It is believed that they result from phase transformations in silicate minerals of the mantle. Using seismic waves that are reflected off the discontinuities, seismologists can also provide regional details on the variations in depth and sharpness of the discontinuities. These observations can provide a wealth of information on the physical and chemical state of the mantle on a relatively local scale. Interpreting these findings, however, requires information on the mineral reactions that cause these discontinuities, which can only be obtained from laboratory experiments.

The 410 km discontinuity, for example, is caused by the transformation of  $(\text{Mg,Fe})_2\text{SiO}_4$  from the olivine to the

wadsleyite structure. The sharpness or width of a discontinuity such as the "410", *i.e.*, the depth interval in the Earth over which it takes place, can provide important evidence for the composition of the mantle in that region. As mantle olivine is a solid solution involving two components,  $\text{Mg}_2\text{SiO}_4$  and  $\text{Fe}_2\text{SiO}_4$ , it is not expected to transform sharply to wadsleyite at a specific depth, but rather the transformation will be smeared out over a broader depth interval. This can be seen in the phase diagram shown in Figure 5.2, which has been calculated using the results of high pressure and temperature multianvil experiments. Because both olivine and wadsleyite contain iron, a two-phase transformation interval is entered where both minerals coexist. For a viable mantle olivine with a  $\text{Fe}_2\text{SiO}_4$  content of 10 % (shown as the dotted yellow line), the transformation will take place over an 8 km wide depth interval. Seismic observations, however, show that in some regions of the Earth the 410 km discontinuity can occur over a 4 km interval, while in other regions it appears broader than 20 km. At Bayerisches Geoinstitut, we are particularly interested in understanding the factors that may cause this type of variation. By performing high pressure and temperature multianvil experiments we can examine the effects of various components and assemblages on the mineral transformations that cause seismic discontinu-

## Mineral phase transformation

ities. There are many factors that may influence the width of mantle discontinuities such as the presence of H<sub>2</sub>O, the redox state in the mantle, the rate of mantle upwelling, and the existence of non-transforming minerals such as garnet. All these factors must be carefully

characterised if we are to extract meaningful information from seismic observations. The 410 km discontinuity is probably strongly affected by water, which is much more soluble in the wadsleyite phase than in olivine. Accordingly, the depth and width of this

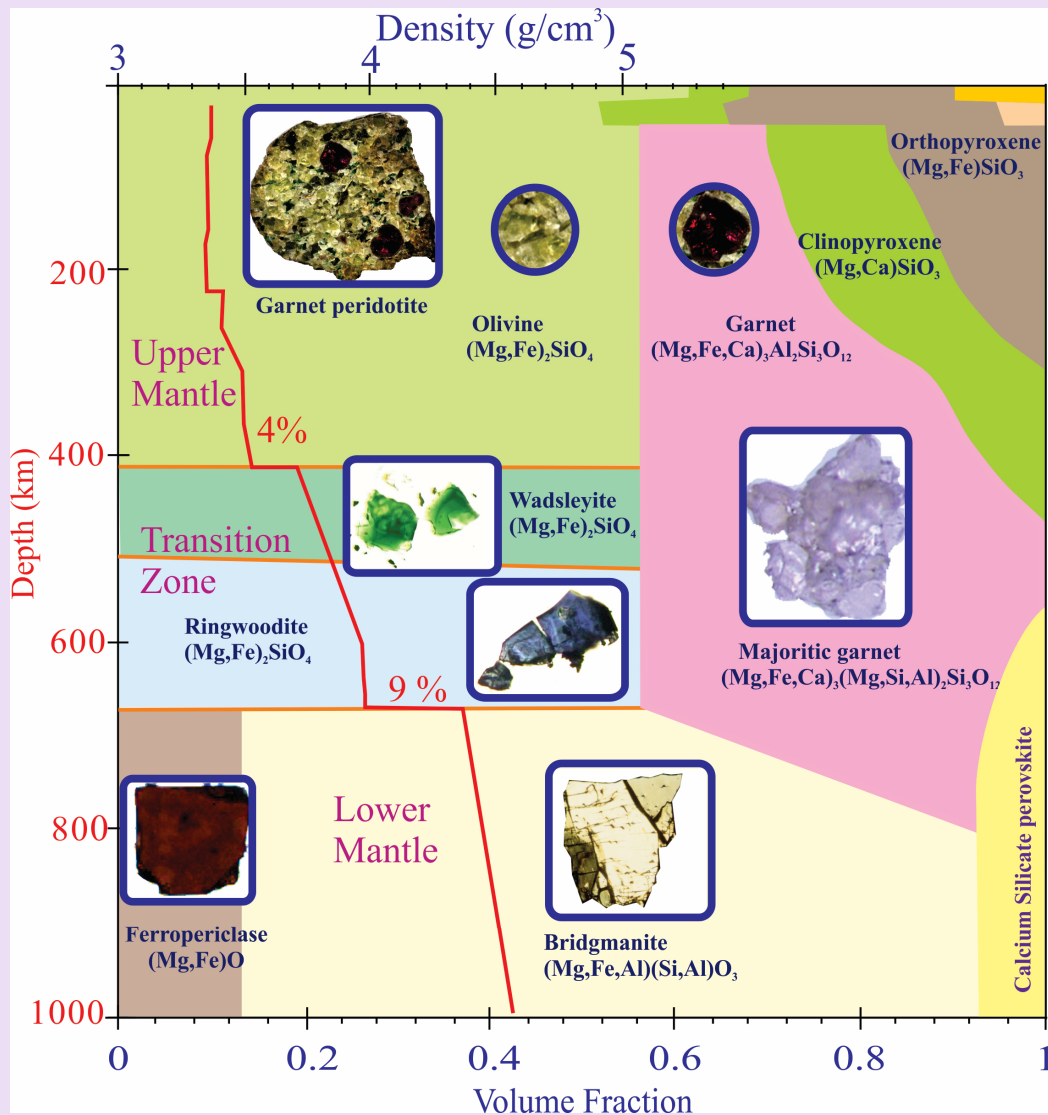


Fig. 5.1: The mineralogy of the Earth's mantle. The coloured fields show the volume fractions of the various minerals of the mantle. In the upper mantle, a garnet peridotite xenolith hand specimen is shown in the inset, which contains olivine, garnet, orthopyroxene and clinopyroxene. The inset diagrams at depths below 400 km show high-pressure minerals recovered from multianvil experiments, with the field of view in each diagram being approximately 0.2 mm across. The red curve indicates the PREM model for the density of the mantle as a function of depth. The 410 km and 660 km discontinuities can be seen with their respective density jumps indicated.

discontinuity may provide insights into the distribution of water in the mantle. The 520 km discontinuity, which is usually assigned to the transformation of wadsleyite to ringwoodite, appears not well resolved in all regions of the mantle, but has also been observed in some parts to be split into two separate discontinuities. Research at Bayerisches Geoinstitut has shown that one of these two discontinuities is due to the formation of  $\text{CaSiO}_3$  perovskite from garnet. Probably, the appearance of this discontinuity is limited to calcium-rich parts of the mantle that contain recycled oceanic crust. Seismic observation of the "520" together with laboratory experiments may therefore allow a chemical mapping of the mantle transition zone.

Some very basic observations of some discontinuities have also yet to be fully explained. The 660-km discontinuity is a very prominent feature, which separates the transition zone from the lower mantle. This discontinuity is attributed to the dissociation of  $(\text{Mg,Fe})_2\text{SiO}_4$  ringwoodite to  $(\text{Mg,Fe})\text{SiO}_3$  bridgmanite and  $(\text{Mg,Fe})\text{O}$  ferropericlasite (Fig. 5.1). The extreme sharpness of this discontinuity is in good agreement with experi-

mental studies at Bayerisches Geoinstitut. However, a detailed study of the 660 km discontinuity under Southeast Africa demonstrated that the depth of the discontinuity varies by more than 30 km within a lateral range of only 200 km. With current mineral physics data, it is very difficult to explain this observation. As more and more detailed seismic observations such as these are reported, therefore the demand for equally detailed and accurate petrological models increases.

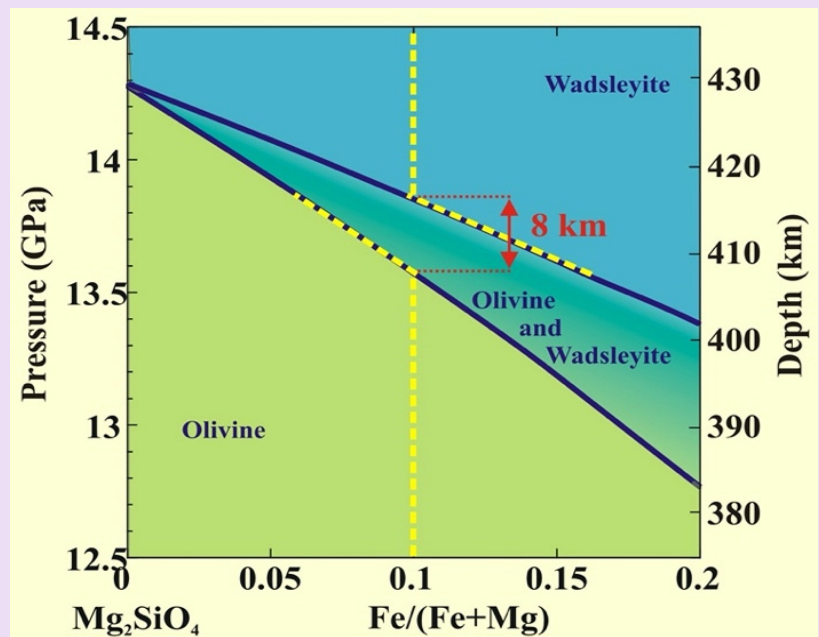


Fig. 5.2: The olivine to wadsleyite transformation, considered to cause the 410 km seismic discontinuity, is calculated in the  $\text{Mg}_2\text{SiO}_4\text{-Fe}_2\text{SiO}_4$  system using a thermodynamic model that was refined from multianvil experiments. The mantle has an olivine  $\text{Fe}/(\text{Fe}+\text{Mg})$  ratio of approximately 0.1, as indicated by the yellow dashed line. This composition is calculated to transform to wadsleyite over a transformation interval of approximately 0.3 GPa or 8 km. In different regions of the mantle the 410 km discontinuity is observed to be broader and sharper than 8 km, which may be due to a number of factors such as the water content, the rate of mantle upwelling and existence of additional minerals such as garnet.

# **6. Volatiles in Earth's interior**



**Earth's deep water cycle.** Earth is the only known planet with oceans of liquid water. Very likely, this water was originally stored in the mantle and was brought to the surface by intense volcanic activity in early Earth history. Research in recent years has shown, however, that the present mantle is by no means dry and that there is also extensive recycling of water into the mantle in subduction zones (Fig. 6.1). There appears to be a deep water cycle, which over billions of years exchanges water between the surface and the mantle, resulting in slow fluctuations of sea level in deep geologic time.

Important for understanding Earth's deep water cycle are data on the maximum amount of water that may be stored in mantle minerals. Several pioneering studies on this subject have been carried out at Bayerisches Geoinstitut. For example, experiments in Bayreuth showed for the first time that the  $(\text{Mg,Fe})_2\text{SiO}_4$  ringwoodite phase in the transition zone of the mantle has the capacity to dissolve more than 2 wt. % of water and should therefore be a major water reservoir in Earth's interior. This prediction was fully confirmed by the recent discovery of a hydrous ringwoodite inclusion in a natural diamond

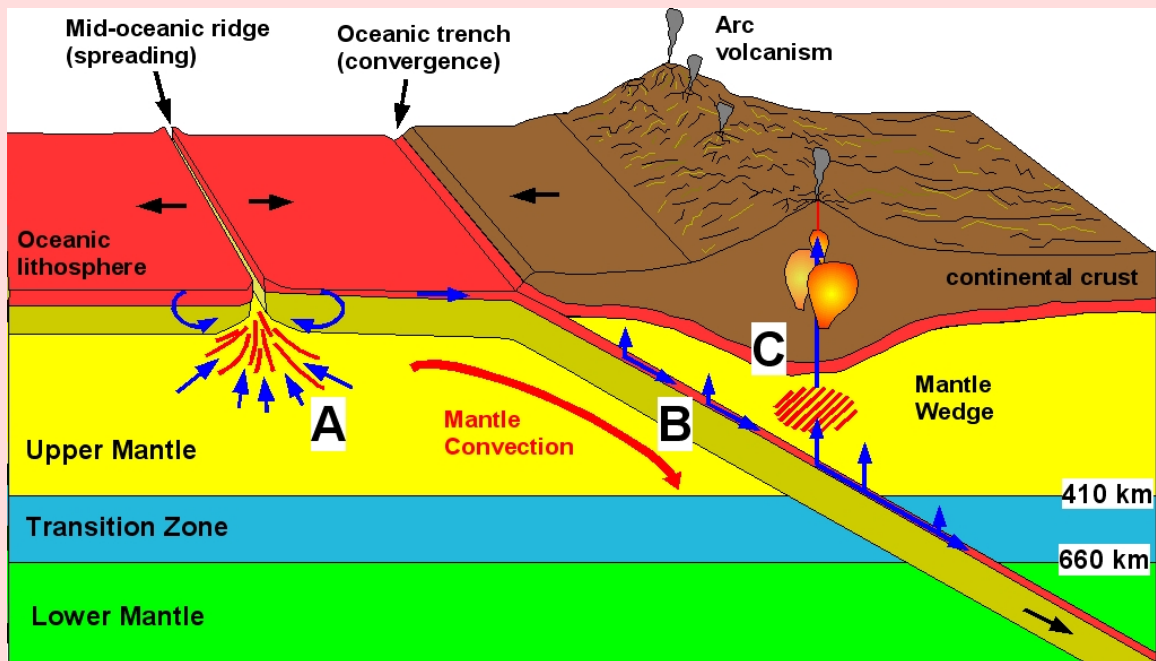


*Fig. 6.1: A schematic view of a subduction zone. Oceanic crust that was produced by melting at mid-ocean ridges (A) was in contact with seawater for millions of years when it is subducted below a continental margin. Some hydrous minerals start to decompose already at shallow depths (B). The hydrous fluids released by this process cause melting in the mantle (C), which feeds arc volcanoes on the surface. Some water, however, is retained in the subducted slab and recycled deep into the mantle.*

## Volatiles in Earth's interior

originating from the transition zone. The ringwoodite in this inclusion contained 1 wt. % of water.

Many of the most active volcanoes on Earth, such as Vesuvius, Mt. Pinatubo or Mt. St. Helens are located in volcanic arcs above subduction zones. When the oceanic crust dives back into the mantle, temperature increases and hydrous minerals become unstable. Water is released as hydrous fluids and causes melting in the mantle wedge above the slab. Already nearly a century ago, scientists suspected that under the corresponding high pressures and temperatures, water and silicate melts may become completely miscible. This effect was for the first time directly demonstrated in Bayreuth; experiments in externally heated diamond cells showed that the phase boundary between water and silicate melt disappears beyond the so-called critical curve (Fig. 6.2). Similar

processes may occur in the mantle deep below arc volcanoes.

**Plate tectonics and melting in the seismic low-velocity zone.** Earth is the only planet in the solar system showing plate tectonics. There is increasing evidence that this unique style of tectonics is also related to the distribution of water in our planet. Plate tectonics appears to require a high viscosity contrast between the stiff lithosphere and the less viscous asthenosphere below it. One idea that had been discussed for decades was that this viscosity contrast is due to differences in the water content in olivine in the lithospheric and asthenospheric mantle. However, recent work in Bayreuth has cast considerable doubt on this hypothesis, as the effect of dissolved water on the mechanical strength of olivine appears to be much smaller than previously thought. More

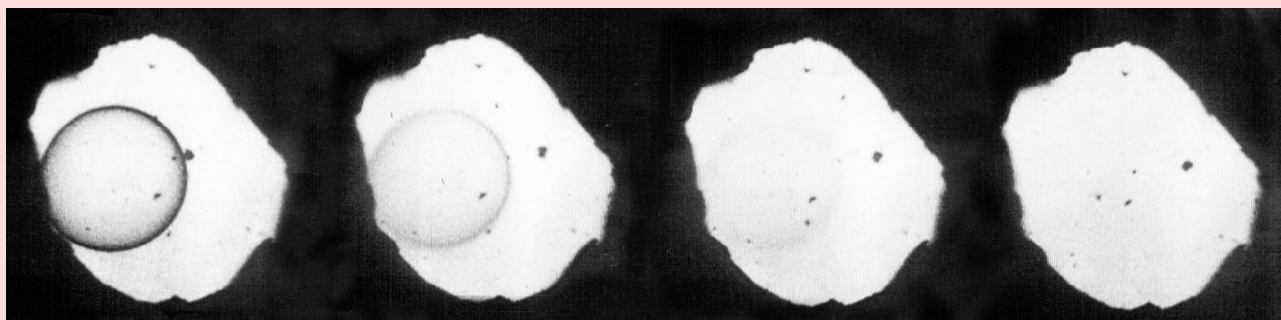


*Fig. 6.2: Complete miscibility between silicate melt and water as seen in an externally heated diamond cell at 1.45 GPa and 763-766 °C. The optical contrast between a droplet of hydrous albite melt and the surrounding fluid disappears as the compositions of the coexisting phases approach each other. The width of the sample chamber shown is about 0.5 mm.*

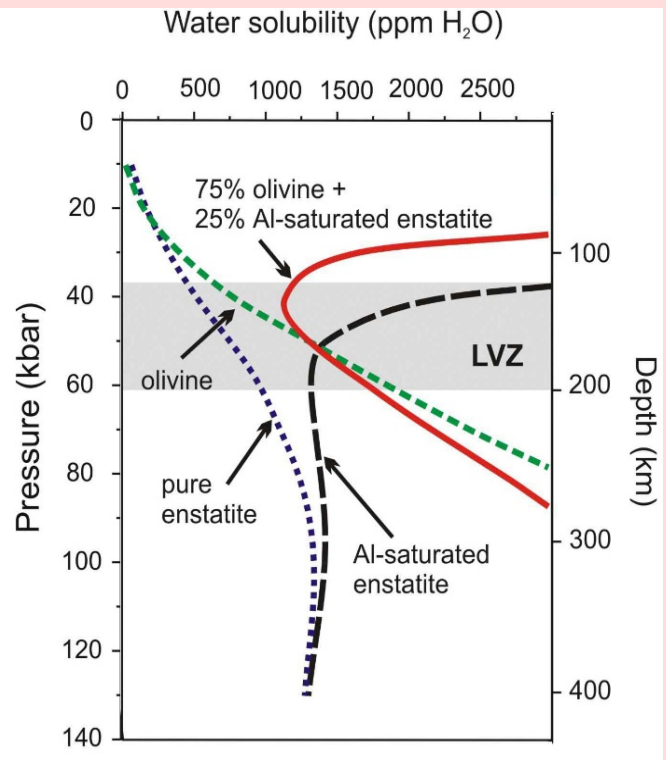
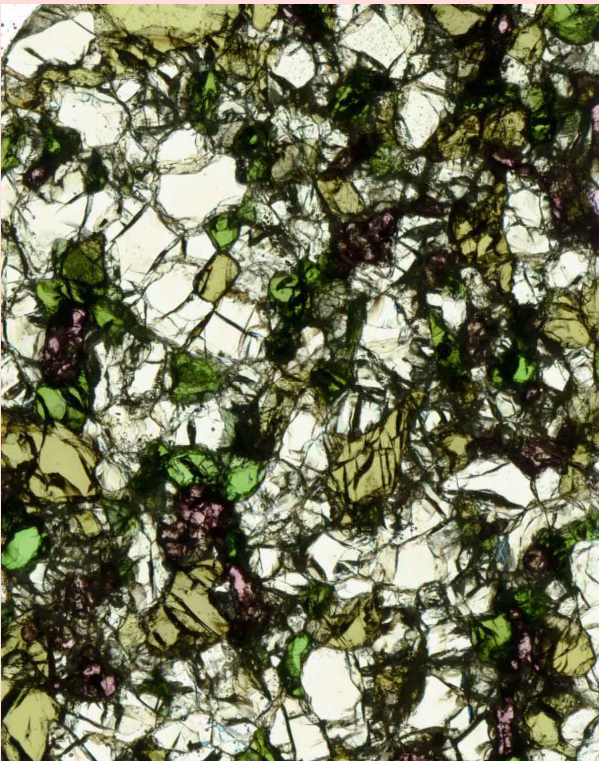


Fig. 6.3: Water solubility in mantle minerals and partial melting in Earth's asthenosphere. A thin section of a peridotite sample from the upper mantle is shown on the left. Main constituents of the mantle are olivine (almost colorless) and orthopyroxene (brownish green). Minor amounts of clinopyroxene (bright green) and garnet (red) are also present. While water solubility in olivine increases with depth (green curve on the right diagram), the solubility in orthopyroxene (black curve) drops sharply. Therefore, bulk water solubility (red curve) has a sharp minimum, which coincides with the seismic low-velocity zone (LVZ). Very likely, the minimum in water solubility in minerals causes water to partition into a small fraction of partial melt.

likely, the low viscosity of the asthenosphere is due to the presence of a small fraction of hydrous silicate melt. Melting in the asthenosphere is likely related to a minimum in the water solubility in mantle minerals; this minimum occurs, because water solubility in olivine increases continuously with pressure, while the water solubility in orthopyroxene, the second most abundant mineral in the upper mantle, sharply decreases with pressure and temperature

(Fig. 6.3). In the region where water solubility is low, water partitions into a small fraction of silicate melt. The presence of some melt greatly reduces viscosity and the velocity of seismic waves travelling through this part of the mantle, while electrical conductivity is increased. All of these effects are in perfect agreement with geophysical observations in the seismic low velocity zone, which is located at a depth between about 100 and 200 km in the mantle.

## Volatiles in Earth's interior

**Carbon in the mantle.** The concentration of carbon dioxide in the atmosphere largely controlled climate on Earth in the geologic past. In the warm periods of the Cretaceous, CO<sub>2</sub> concentrations were likely about ten times higher than today. This is because the by far largest carbon reservoir on Earth is the mantle and a slight imbalance between volcanic outgassing and carbon withdrawal from the atmosphere by weathering and burial of carbon can cause major shifts in climate. There is increasing evidence that major mass extinction events in Earth history are linked to gigantic flood basalt eruptions that released massive amounts of

carbon, sulfur, and chlorine from Earth's mantle to the atmosphere. The mode of carbon storage in the mantle is therefore of fundamental importance for understanding the long-term evolution of atmospheric composition and climate on Earth. Research at Bayerisches Geoinstitut has, among other things, clarified the carbon storage capacity of olivine and other major mantle minerals. Figure 6.4 shows olivine crystals that were crystallised from a carbonate melt, so that they were certainly carbon-saturated. Chemical analyses by secondary ion mass spectrometry showed that the carbon content in these crystals is exceedingly low, reaching only fractions

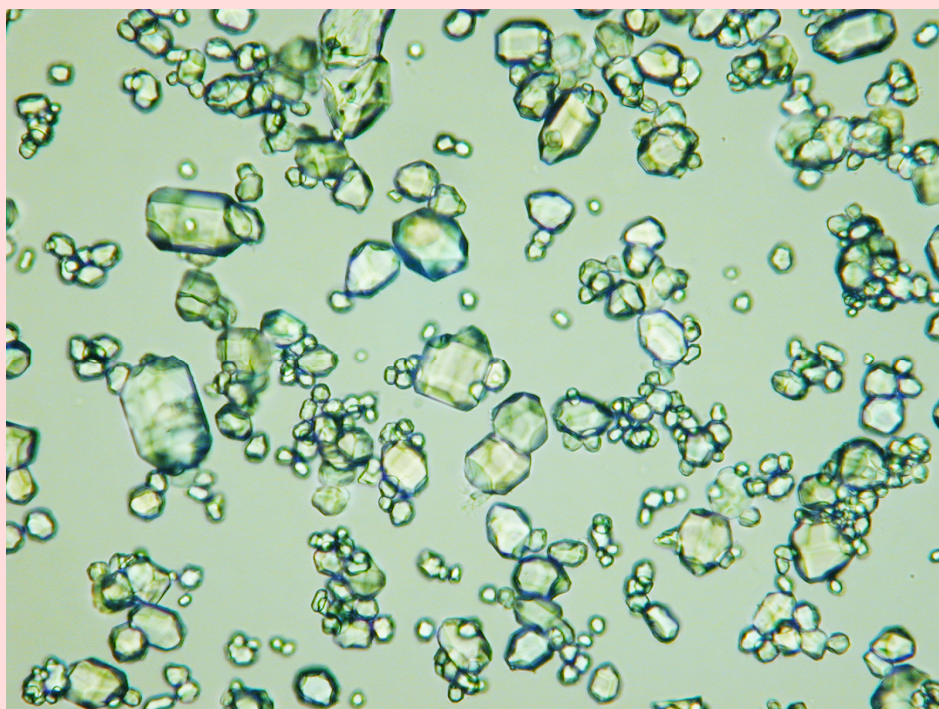


*Fig. 6.4: Facetted crystals of olivine, crystallised from a carbonate melt. The carbon content in these olivines was found to be below the ppm level, implying that carbon in the mantle is mostly stored in accessory phases, such as carbonates.*

of a ppm in the uppermost mantle. An important consequence of this observation is that carbon in the mantle must be stored in a separate phase, most likely carbonate in the uppermost mantle and diamond or carbides in the deeper mantle. Since carbonates have very low melting points and the melts are very mobile, this opens the possibility of a sudden release of large amounts of carbon to the atmosphere.

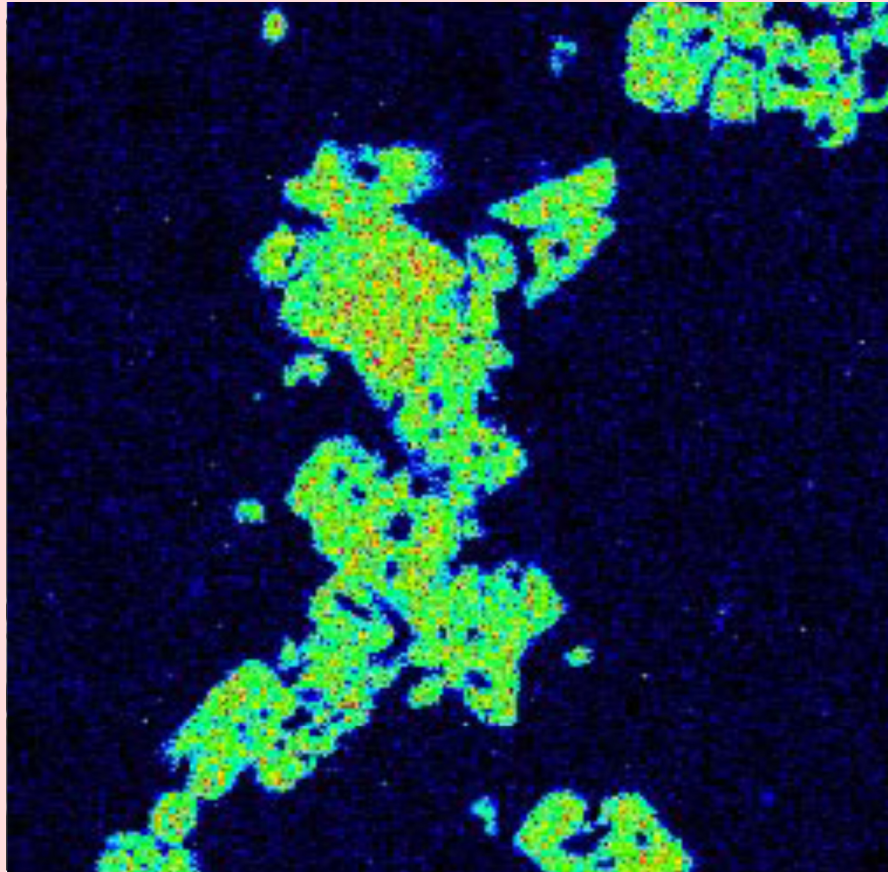


*Fig. 6.5: An X-ray map of argon in a sample containing crystals of argon-saturated phase X in a matrix of MgSiO<sub>3</sub> akimotoite. The green colour corresponds to about 0.5 wt. % of argon. The width of the image is about 0.1 mm.*

**Noble gases and nitrogen: The origin of the atmosphere.** The abundance of noble gases on Earth likely contains information on the early history of our planet. One important observation is that the xenon isotopes that must have been produced by the radioactive decay of plutonium-244 in the early stages of Earth history seem to have largely disappeared from our planet. This suggests that some events of vigorous mantle outgassing and of atmospheric loss must have occurred shortly after the formation of the Earth. Other xenon

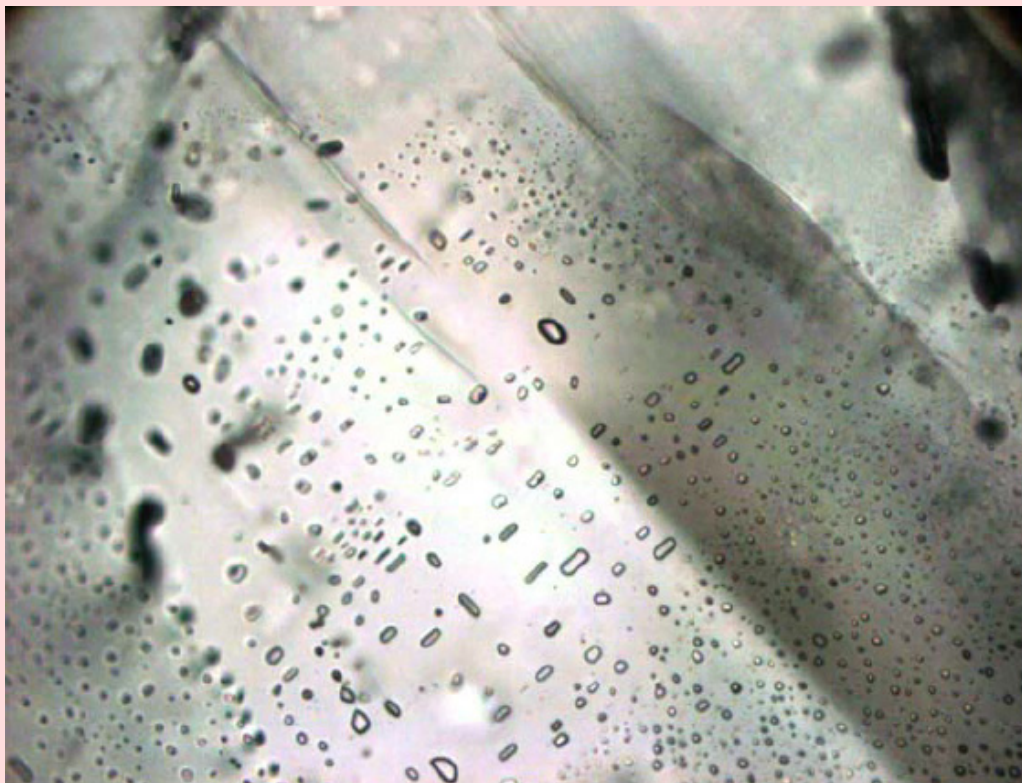
isotopes are also quite rare on Earth, if compared to argon. This problem of "missing xenon" has puzzled geochemists since decades. A number of experimental studies had been carried out, which showed that all noble gases are extremely insoluble in upper mantle minerals. However, the solubility of noble gases in lower mantle minerals was for the first time investigated at Bayerisches Geoinstitut. These experiments showed that argon, but not xenon, is highly soluble in MgSiO<sub>3</sub> bridgmanite.

Argon solubility reaches up to 1 wt. %, likely because the Ar atom fits well into oxygen vacancies in the bridgmanite structure. Xenon is too large for these vacancies. This concept was confirmed by the observation of high Ar solubilities in phase X, a silicate with a layer structure and abundant potassium vacancies (Fig. 6.5). The experimental data suggest a simple explanation for the relative abundance of argon and xenon on Earth: when bridgmanite crystallised from a global magma ocean in equilibrium with a primitive atmosphere, it sequestered argon, but not xenon in its crystal structure. Most of the atmosphere was then lost by heavy impacts and meteorite bombardment on the surface. Later degassing of the mantle then replenished argon, but not xenon in the atmosphere. This simple model not only explains the depletion of xenon relative to argon, but it can also account for the relative abundance of noble gas isotopes.

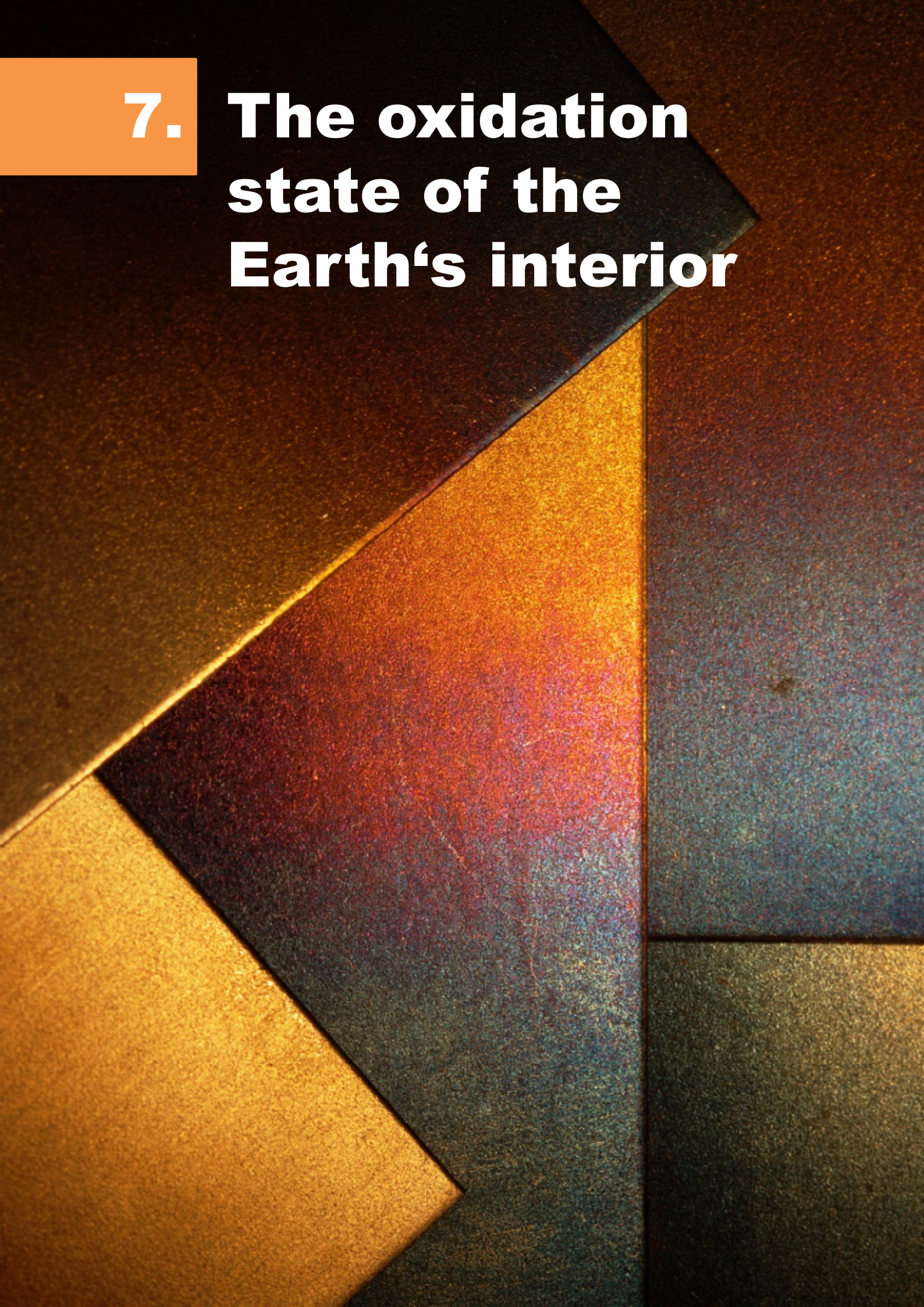
Just like the oceans, most of the present atmosphere likely formed by degassing of the mantle. Air contains 78 % of  $N_2$ , but how nitrogen could be stored in the mantle and what could have caused nitrogen degassing was poorly understood until recently. Research in Bayreuth showed that nitrogen solubility in mantle minerals is greatly

enhanced under reducing conditions. Accordingly, the degassing of nitrogen in early Earth's history may have been related to the oxidation of the mantle.

**Immiscibility between water and hydrogen.** The first step in the origin of life probably was the abiotic formation of biomolecules by Miller-Urey type reactions. Amino acids and many other molecules essential for life can be produced by electrical discharges in  $NH_3$ - $CH_4$ - $H_2O$  mixtures. However, the viability of this mechanism for forming biomolecules on early Earth has been questioned, because it would require a very reducing early atmosphere, which is unstable due to the loss of hydrogen to space. This problem could perhaps be solved by an observation that was made by accident in the course of experimental studies in Bayreuth. Experiments showed two types of fluid inclusions trapped by olivine crystals under reducing conditions (Fig. 6.6): inclusions consisting of nearly pure water coexisted with inclusions that contained nearly pure  $H_2$ , as identified by Raman spectroscopy. These results imply that  $H_2$  and  $H_2O$  are immiscible in Earth's upper mantle. The immiscibility could have caused the extensive degassing of nearly pure  $H_2$ , which may have stabilised a very reducing atmosphere in early Earth history.



*Fig. 6.6: Immiscibility between water and hydrogen as seen in fluid inclusions in olivine, trapped at 2.6 GPa and 1000 °C. Bright fluid inclusions contain nearly pure water, while the dark fluid inclusions contain nearly pure hydrogen (H<sub>2</sub>), as confirmed by Raman spectroscopy. The two pictures show different regions of the same olivine crystal.*

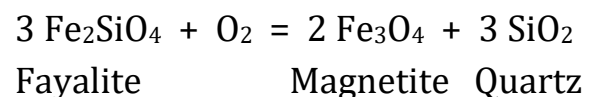
The background features a complex geometric composition. A large, dark, textured triangle points downwards from the top left. The rest of the space is filled with various shades of brown, gold, and blue, separated by sharp, angular lines. The overall effect is that of a textured, layered surface, possibly representing geological strata or a cross-section of the Earth's interior.

# **7. The oxidation state of the Earth's interior**

Depending on the availability of oxygen, elements such as carbon, sulphur and iron will exist in different oxidation states in the Earth's interior. Iron for example, exists as a metal in the Earth's core, but is predominantly present as ferrous iron ( $\text{Fe}^{2+}$ ,  $\text{FeO}$ ) in minerals of the upper mantle. Similarly, volatile elements such as carbon can exist under certain conditions bonded to oxygen, such as in  $\text{CO}_2$ , but under oxygen-poor conditions they exist in so-called reduced forms, such as diamond or graphite. Consequently, to understand the compositions of mineral and volatile phases stable under different conditions, the amount of oxygen in the system needs to be also taken into account. Defining a bulk oxygen concentration is relatively unhelpful in this case, as this varies more strongly as the proportions of oxides such as  $\text{SiO}_2$  and  $\text{MgO}$  change. The speciation of elements with varying oxidation states are more easily described with reference to the oxygen fugacity ( $f\text{O}_2$ ). At low oxygen fugacities iron will tend to form a metal and reduced, oxygen-free volatile components such as  $\text{H}_2$ ,  $\text{CH}_4$  or  $\text{H}_2\text{S}$  are stable. At higher oxygen fugacities, iron metal is unstable and minerals will start to contain ferric ( $\text{Fe}^{3+}$ ,  $\text{Fe}_2\text{O}_3$ ) iron in addition to the normally more dominant ferrous iron (Fig. 7.1). As the incorporation of ferric iron into minerals is often associated with the formation of lattice

defects, its presence can have a strong influence on physical properties such as cation diffusion, dislocation creep and electrical conductivity, which are in turn then also dependent on oxygen fugacity.

Determining the prevailing oxygen fugacity in the mantle is therefore important in terms of constraining physical properties and volatile speciation within the Earth. Furthermore, the oxygen fugacity of a mantle-derived melt will influence the extent to which it degasses as it approaches the surface, which can have a strong influence on the style of volcanic eruptions. The oxygen fugacity of a rock from the mantle can be measured by considering an equilibrium between mineral components containing iron in different oxidation states, such as



By measuring the proportions of these components in the minerals of a mantle rock, the oxygen fugacity can be calculated, once certain thermodynamic properties of the equilibrium have been determined. When this particular equilibrium is considered for an assemblage of the pure phases it defines the so-called fayalite-magnetite-quartz (FMQ) oxygen buffer, which is used as a

## The oxidation state of the Earth's interior

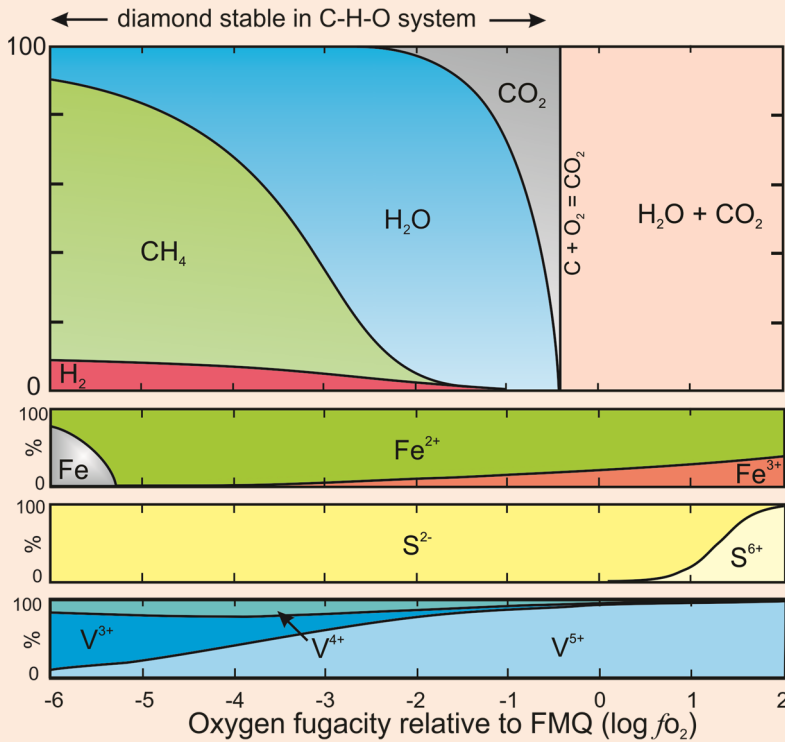


Fig. 7.1: The composition of a C-O-H fluid in equilibrium with diamond as a function of oxygen fugacity at conditions equivalent to 180 km depth in the Earth (top graph). The lower three graphs show proportions of the different oxidation states of iron, sulphur and vanadium species dissolved in silicate melts (except the grey Fe metal field which forms an immiscible phase) at conditions equivalent to approximately 90 km depth.

reference state for oxygen fugacity. Calibrating such equilibria for use on mantle rocks is an important task in high-pressure Earth sciences, which furthermore requires the accurate determination of the ferric-ferrous ratio of mineral phases. This can be accomplished using Mössbauer and electron energy loss spectroscopies but becomes challenging as a result of the small size of high-pressure experimental products.

Calibrations also exist to allow the oxygen fugacity of erupted lavas to be

determined from measurements of their ferric-ferrous ratios. However, in ancient lavas flows these ratios can be easily affected by alteration processes. In such instances constraints can be placed on the oxygen fugacity of the original magmas by considering their concentrations of elements less prone to alteration such as vanadium, which also enter melts in different proportions depending on their oxidation state (Fig. 7.1).

Rocks and magmas from various tectonic settings exhibit important differences in oxygen fugacities (Fig. 7.2). Magmas from mid-ocean ridges

for example indicate oxygen fugacities close to the FMQ oxygen buffer consistent with the degassing of  $CO_2$  and  $H_2O$ . Rocks brought to the surface by subduction zone-related magmas can often exhibit even higher oxygen fugacities, likely related to the subduction and release of oxidised fluids in the mantle above subducting slabs. Rocks from the thick cratonic mantle, such as that which underlies much of South Africa or Canada, exhibit lower oxygen fugacities consistent with the presence of diamonds in some of these assemblages.

Diamonds most likely form as a result of reduction of  $\text{CO}_2$  species in metasomatic fluids or melts. This might include melts not unlike the kimberlite magmas that bring them to the surface. However, it is also possible that some diamonds are formed as a result of the oxidation of  $\text{CH}_4$ -bearing fluids.

Experimental studies at Bayerisches Geoinstitut have focused in recent years on understanding the oxygen fugacity at depths in the mantle from which no rock samples are available. Such studies indicate that the oxygen fugacity will tend to decrease with increasing depth in the Earth, as a result of the effect of increasing pressure on ferric-ferrous iron reactions between mineral phases. This effect will result in the removal of oxygen from volatile species such as  $\text{CO}_2$  in order to oxidise  $\text{FeO}$  in mineral phases to  $\text{Fe}_2\text{O}_3$ , with the result that diamond will be the predominant form of carbon in the mantle at depths greater than 250 km. Conversely, as mantle rocks upwell beneath mid-ocean ridges, the opposite reaction will occur to produce  $\text{CO}_2$  from diamond. As the formation of  $\text{CO}_2$  at such depths will lower the melting temperature of rocks, a so-called redox melting

event likely takes place where the decompression-induced oxidation of diamond leads to the instigation of mantle melting. A complementary process, termed redox freezing may occur above subducting oceanic crust when  $\text{CO}_2$ -rich melts or fluids enter the more reduced overlying mantle and form diamond. At conditions approaching the lower mantle the oxygen fugacity may be low enough for iron carbide minerals to form such as  $\text{Fe}_3\text{C}$ . In the lower mantle ( $> 660$  km) these minerals may be also joined by metallic iron, depending on the amount of carbon present.

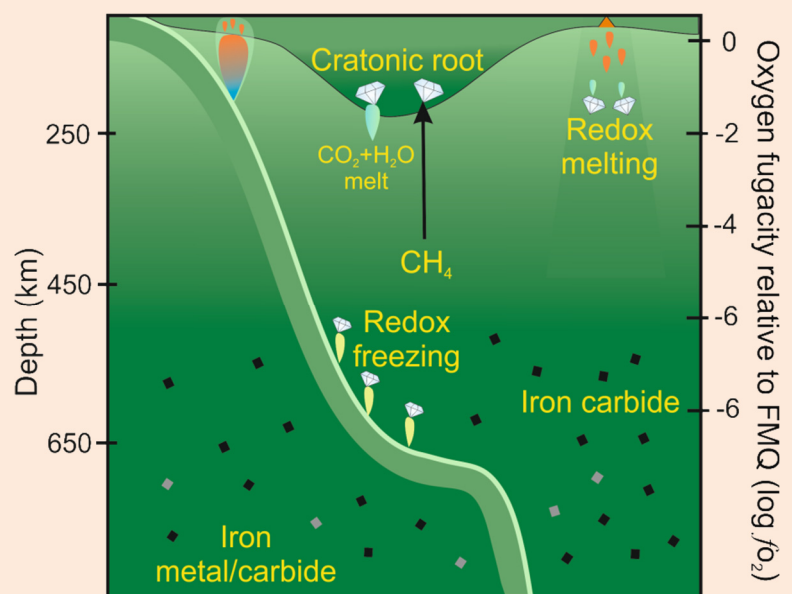


Fig 7.2: The variation in oxygen fugacity in the mantle as a function of depth and tectonic setting as indicated by the shading: light green most oxidised, dark green most reduced. Oxygen fugacity will tend to decrease with depth in the interior as a result of the effect of pressure on ferric-ferrous iron reactions in mantle minerals. This will cause oxygen-free volatile-bearing phases to be present at depth, such as  $\text{CH}_4$  or iron carbide ( $\text{Fe}_3\text{C}$ ). Conditions in the lower mantle may be sufficiently reducing for around 1 wt. % Fe-metal to exist.

# 8. Mantle convection and rheology

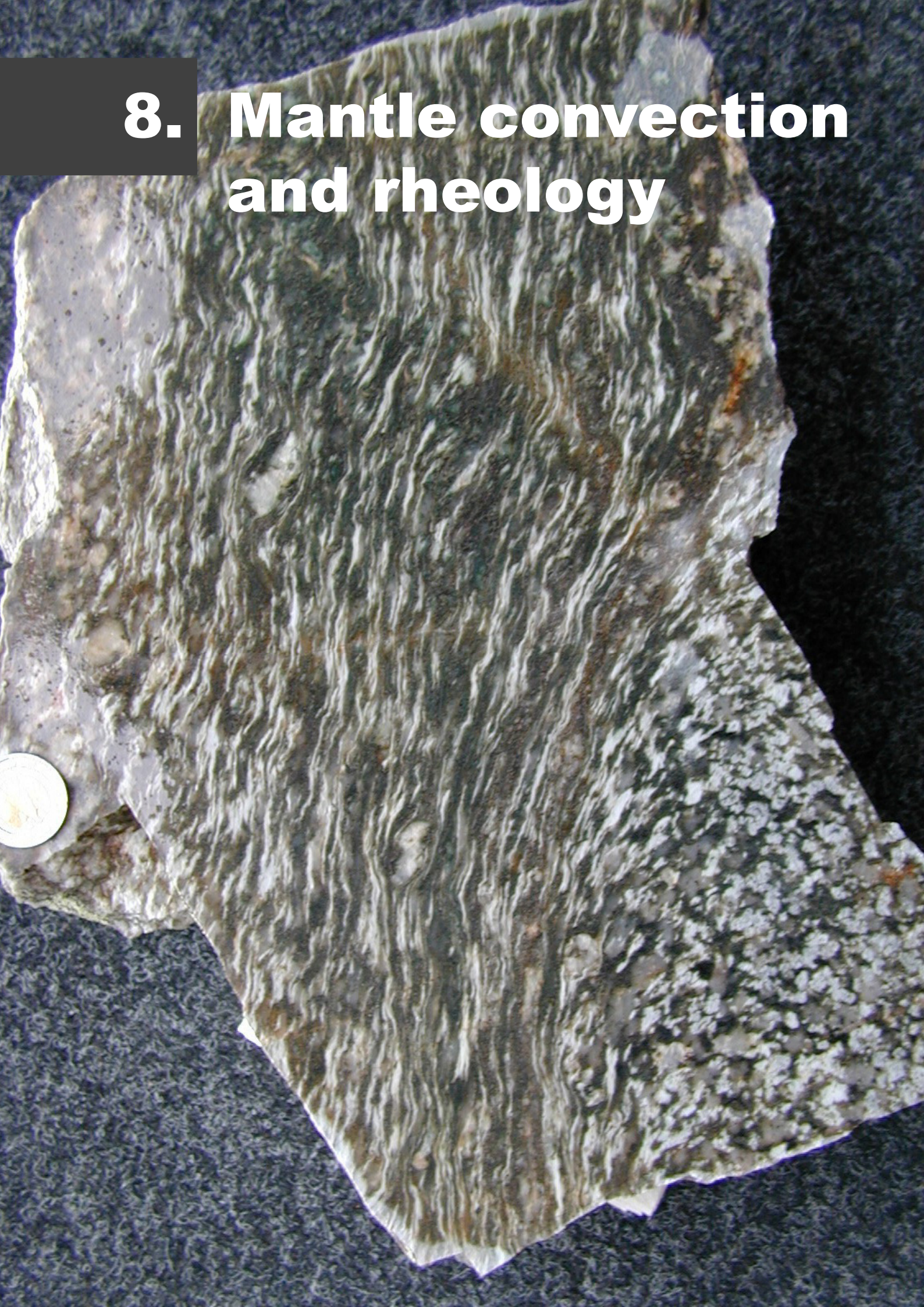
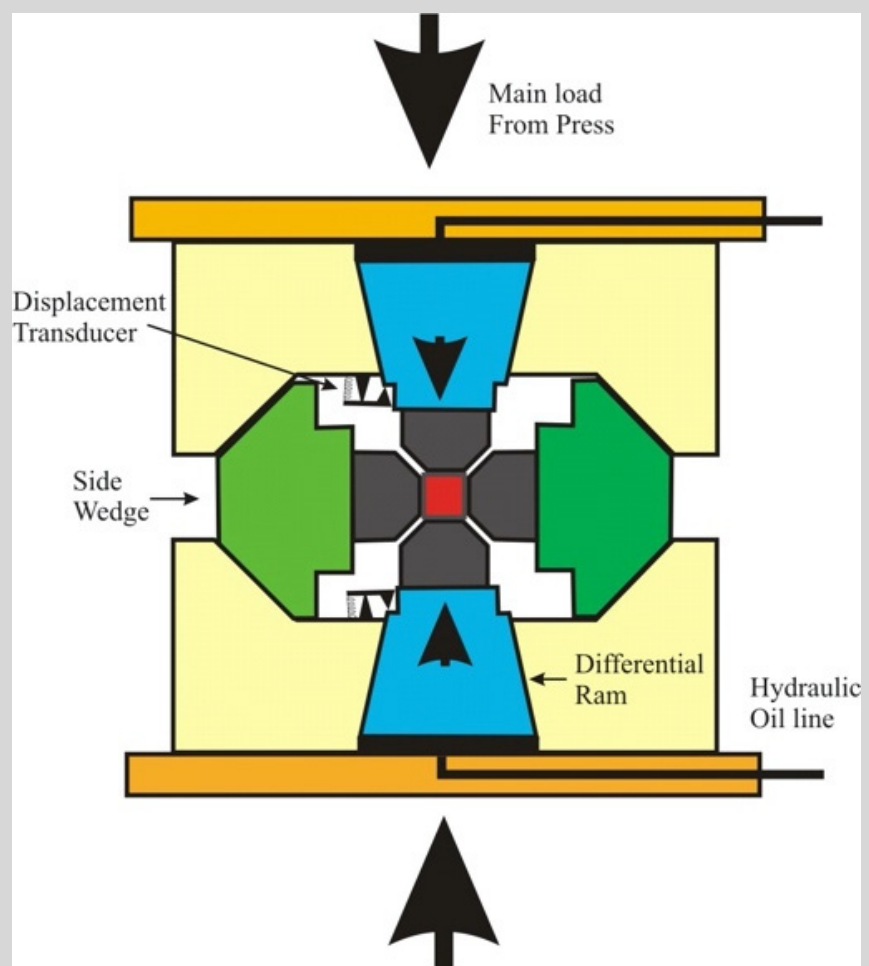


Plate tectonics, earthquakes, volcanic eruptions, and many other processes on Earth's surface are driven by mantle convection. Due to the high pressures and temperatures, the rocks in the mantle behave plastically, *i.e.*, they can be deformed while remaining in the solid state. Over long geological time scales, the mantle convects by material rising from the hot core-mantle interface to the upper mantle and returning to great depth. This is the main interior engine of the Earth, which transports heat from the hot core to the cool surface. The determination of the rheology of Earth materials (*i.e.*, their mechanical response to applied stresses and strains) is therefore crucial to understanding the Earth's interior. The rheology of minerals and rocks is described by flow laws, which relate the applied stresses to the deformation rates. Many additional factors such as temperature, pressure, grain size, oxygen fugacity and water content may affect the flow law of a material. At Bayerisches Geo-

institut, we attempt to determine the flow laws of the most common phases of the Earth's interior by recording their mechanical response to applied stresses under controlled experimental conditions. High-pressure deformation experiments may be carried out with the D-DIA press (Fig. 8.1), or with the six-axis press developed at Bayerisches Geoinstitut (see Fig. 2.4 in Chapter 2), which both allow separate control of confining pressures and differential stress.



*Fig. 8.1: The D-DIA press for deformation experiments. The differential stresses can be controlled independently from the confining pressure due to the separate movement of the anvils marked in blue.*

## Mantle convection and rheology

Perfect crystals would not easily deform under stress. Minerals, however, contain line defects in their crystal structures that enhance deformation through so-called dislocation creep. Moreover, in rocks consisting of various mineral grains, deformation may occur through element diffusion on grain-boundaries (diffusion creep).

Since the formation of dislocations depends on the crystal structure, dislocation creep is strongly anisotropic. Deformation therefore causes some preferred orientation of crystals in a rock as

frequently observed, *e.g.*, in metamorphic schists. Since crystals are elastically anisotropic, this means that the velocities of seismic waves travelling through a rock with some preferred orientation of mineral grains will also depend on direction. By observing this "seismic anisotropy" it is therefore possible to reconstruct the texture of rocks and the convection patterns deep in the mantle. A correct interpretation of seismic data, however, requires the calibration by deformation experiments in the laboratory.

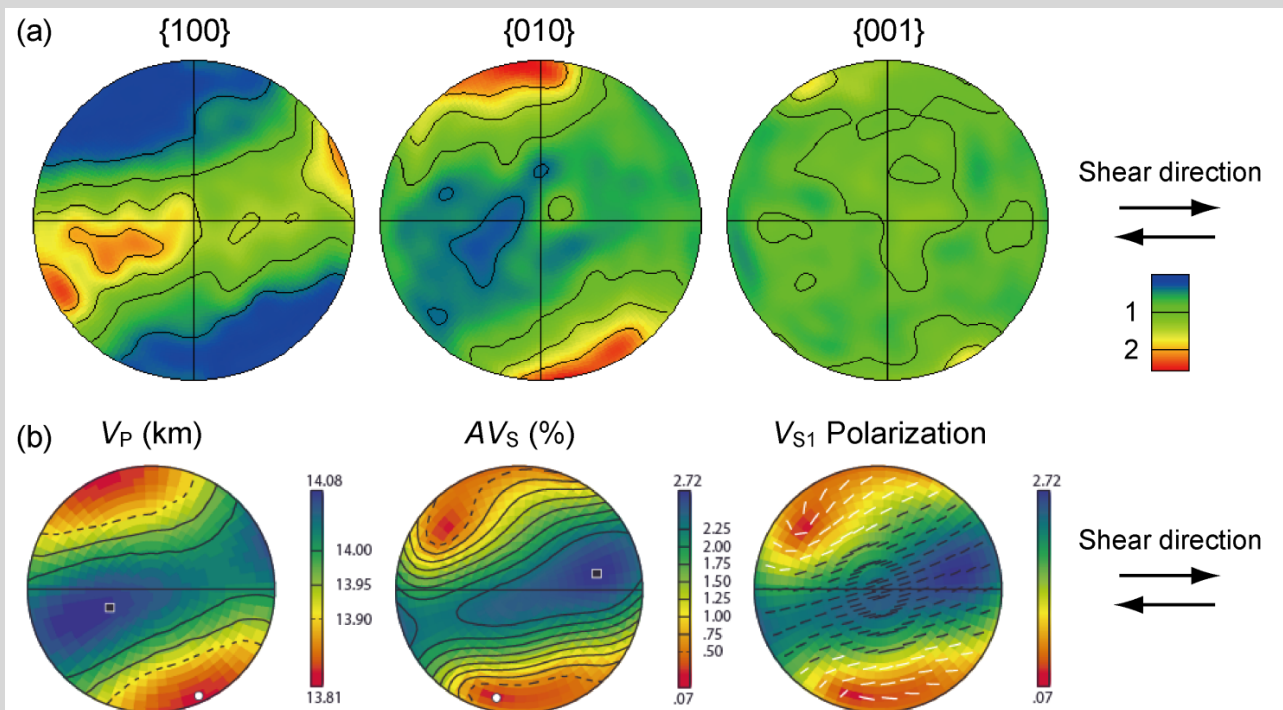
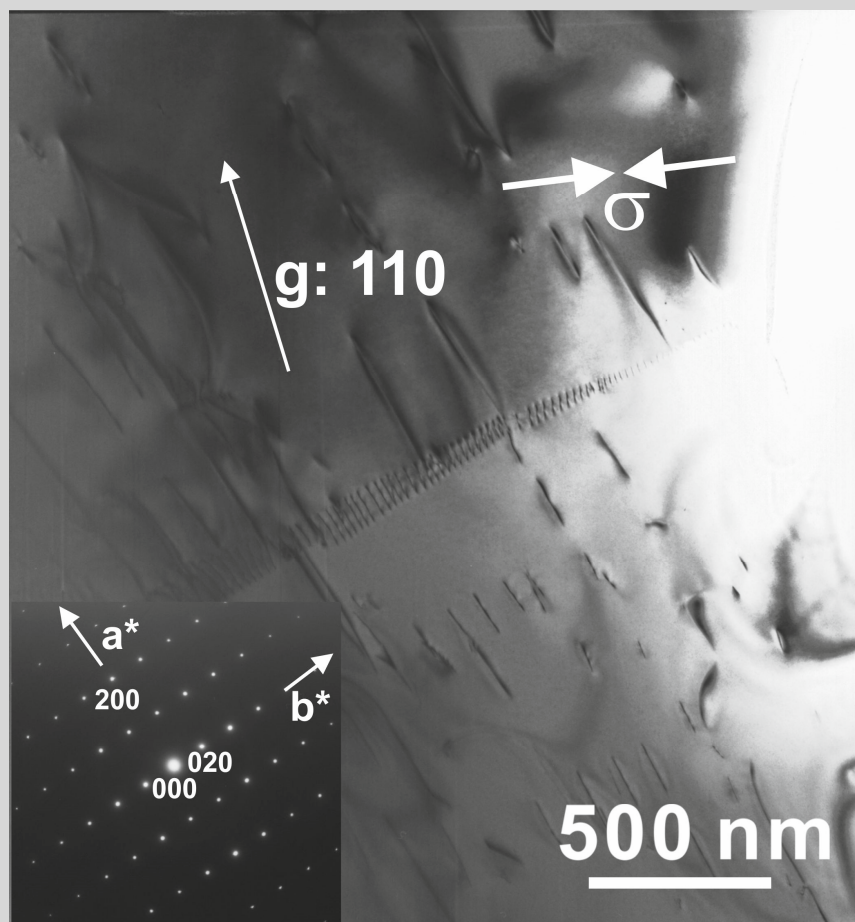


Fig. 8.2: Deformation textures of  $\text{CaIrO}_3$  post-perovskite deformed at 3 GPa and 1273-1473 K. (a) Pole figures showing the preferred orientation of crystals in certain directions for a sample deformed with a shear strain of  $\sim 80\%$  at a strain rate of  $3 \times 10^{-4} \text{ s}^{-1}$ . (b) The seismic anisotropy of the sample shown in (a). Both diagrams are pole figures with lower hemisphere projections. Abbreviations:  $V_P$ , compressional-wave velocity;  $AV_s$ : anisotropy strength;  $V_{S1}$ , fast shear-wave velocity.

Strong seismic anisotropy has been observed at the bottom region of the mantle (so-called D" layer). The seismic anisotropy is thought to be due to the deformation-induced preferred orientation of  $(\text{Mg,Fe})\text{SiO}_3$  post-perovskite, the major mineral in the D" layer. Figure 8.2 shows the grain orientation pattern and seismic anisotropy of a structural analogue of  $(\text{Mg,Fe})\text{SiO}_3$  post-perovskite deformed in the laboratory. By comparing these data with the seismic anisotropy observed in the D" layer, one may

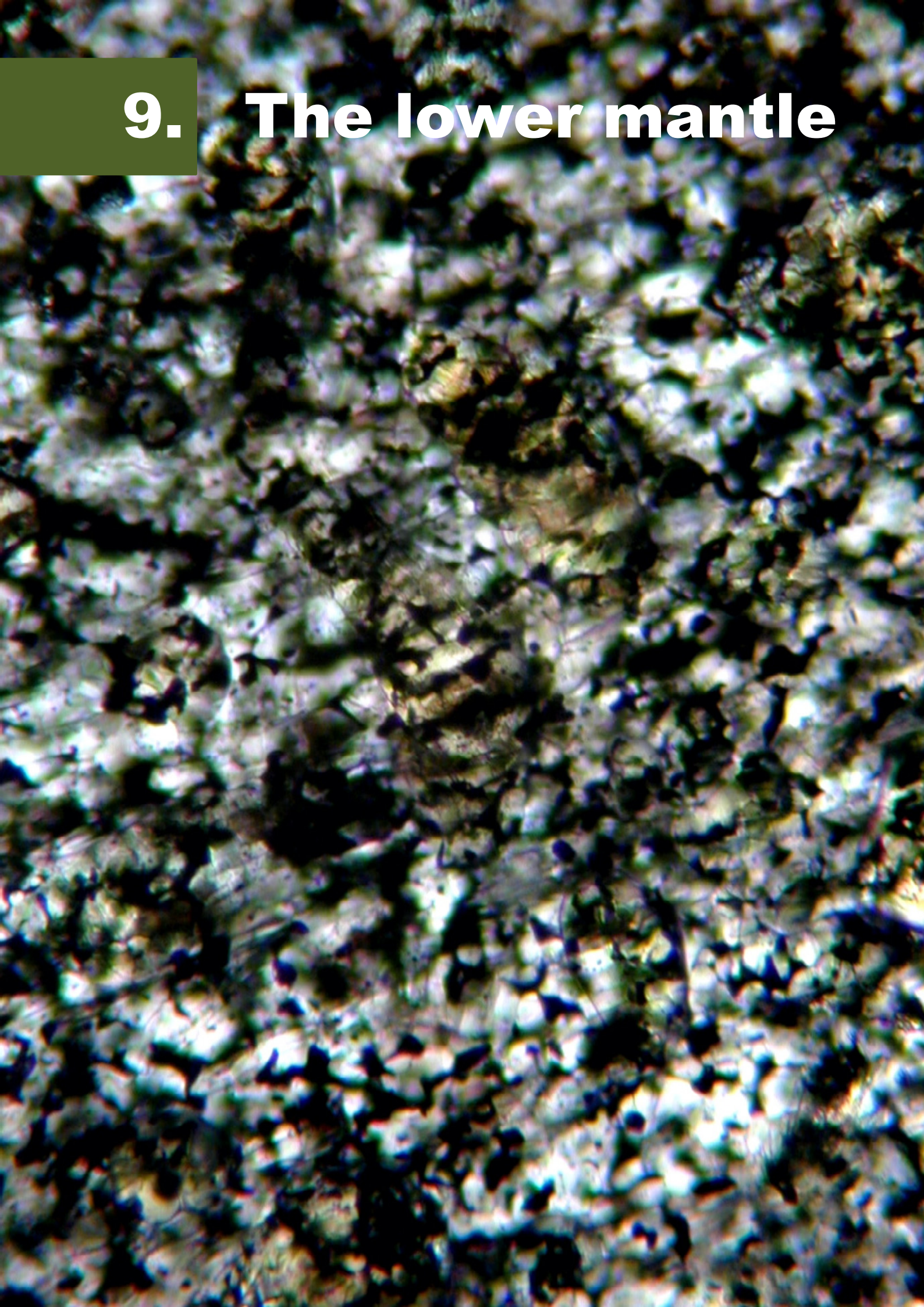
conclude that mantle convection causes horizontal shear flow at the bottom of the mantle.

Seismic anisotropy developed during deformation will depend on the direction in which dislocation glide within the crystal occurs, the so-called slip system. The slip system of a sample may be investigated by transmission electron microscopy (TEM), which allows the direct observation of dislocations (Fig. 8.3).



*Fig. 8.3: A bright-field TEM micrograph of  $\text{CaIrO}_3$  post-perovskite deformed with a uniaxial strain of 50 % at a strain rate of  $3 \times 10^{-5} \text{ s}^{-1}$ . Black lines are dislocations. The inset is a selected-area electron diffraction pattern. The opposing arrows ( $\sigma$ ) indicate the direction of the compression axis.*

# 9. The lower mantle



High-pressure experiments over the past four decades have shown incontrovertible evidence that Mg-rich silicate with perovskite structure (ideally  $\text{MgSiO}_3$ ) is the dominant mineral (about 60 to 80 %) of the lower mantle. Since the Earth's lower mantle constitutes some 55 % (by volume) of the Earth,  $\text{MgSiO}_3$ -rich perovskite is considered to be the most abundant mineral in the Earth. Until recently, however, the phase had no mineral name because of its instability at low pressures that precluded survival in terrestrial rocks. Even when exhumed from the lower mantle within the protective environment of diamond (Fig. 9.1), its crystal structure does not survive. However, the transient high pressures and temperatures generated during shock events in meteorites provide ideal conditions for preservation of high-pressure polymorphs, and indeed the recent characterisation of  $\text{MgSiO}_3$ -rich perovskite in the Tenham meteorite finally brought a mineral name to the Earth's most abundant phase – "bridgmanite" after Percy Bridgman who won the 1946 Nobel Prize in Physics for his work on the physics of high pressures.

The lower mantle is seismically homogeneous over most of its depth compared to other parts of the Earth. Comparisons of laboratory-based measurements of elastic properties and densities with profiles derived from seismology show the lower mantle to consist of a mixture of bridgmanite with smaller amounts of ferropericlase,  $(\text{Mg,Fe})\text{O}$ , and Ca-rich silicate perovskite (ideally  $\text{CaSiO}_3$ ), see Fig. 9.2. The several hundred kilometres immediately above the core-mantle boundary, however, the so-

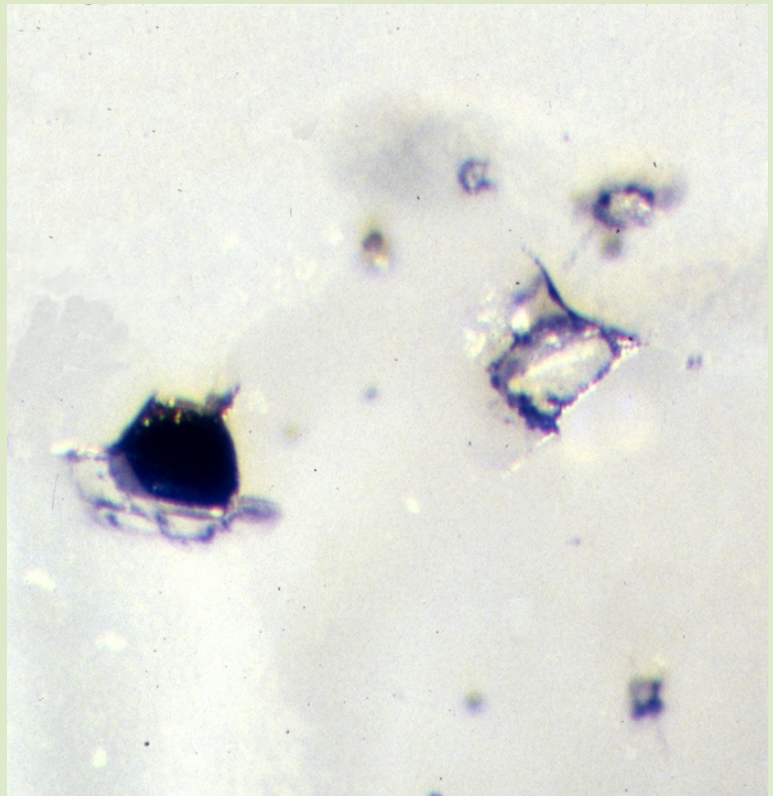


*Fig. 9.1: Diamonds originating in the lower mantle have been sometimes found to contain inclusions of ferropericlase (black) and former bridgmanite (transparent). The latter phase was transformed upon exhumation to pyroxene, but the chemistry was preserved. The field of view is approximately 0.6 mm across.*

## The lower mantle

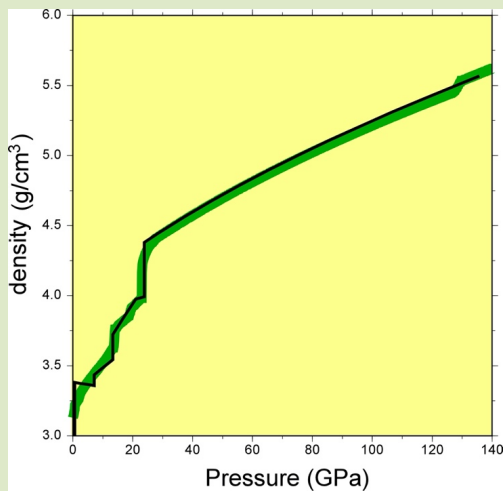


Fig. 9.2: A simulated profile based on densities of lower mantle minerals measured in the laboratory (green line) closely matches the Preliminary Reference Earth Model (black line) derived from seismology.

called D" layer, describe a region of seismic velocity anomalies that cannot be reconciled with this model.

The D" layer marks the boundary between the Earth's rocky mantle and

liquid iron core. Although it is remote, it is one of the most profound interfaces within the Earth and plays a critical role in the Earth's thermal and chemical evolution. Furthermore, processes at the core-mantle boundary can influence the Earth's surface. For example, plumes originating at the core-mantle boundary are thought to manifest themselves as hot-spot volcanoes on Hawaii. For many years, bridgmanite was believed to be stable to pressures and temperatures down to the base of the lower mantle, but in 2004 a structural phase transition was discovered at pressures of the D" layer that helped to explain many of the seismological enigmas of this region. The crystal structure of "post-perovskite" (the high-pressure modification of bridgmanite) is unlike the perovskite structure (Fig. 9.3), so many physical

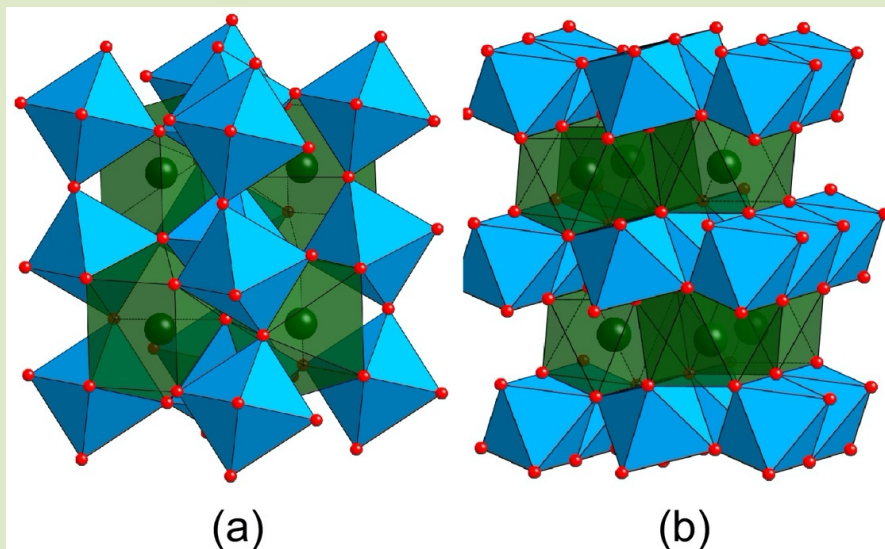


Fig. 9.3: (a) The perovskite structure consists of corner-shared  $\text{SiO}_6$  octahedra (blue) that form a framework around Mg atoms (green). (b) The post-perovskite structure is a denser framework of edge- and corner-linked  $\text{SiO}_6$  octahedra layered in sheets between Mg atoms. Oxygen atoms are shaded red.

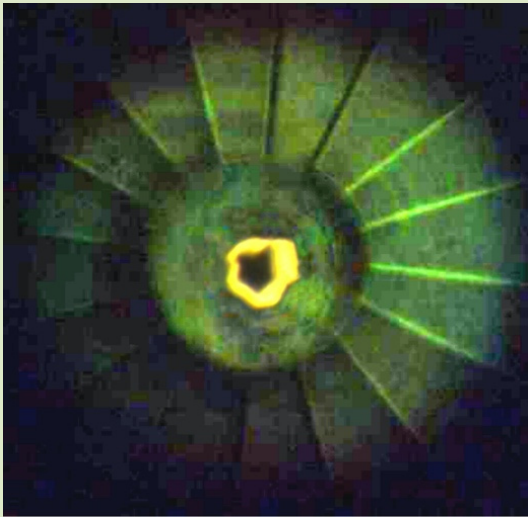


Fig. 9.4: Post-perovskite formed from bridgmanite can only be viewed inside a diamond anvil cell. The crystal is approximately 10  $\mu\text{m}$  across.

and chemical properties of post-perovskite are expected to be different. However post-perovskite is not quenchable,

so all properties must be measured *in situ* using, for example, in a diamond anvil cell (Fig. 9.4).

Physical and chemical properties of lower mantle minerals are affected not only by structural transitions, but also by changes in electronic structure. Iron is of particular interest, since variations in pressure or temperature can cause changes in the number of electrons (oxidation state) or in the distribution of electrons (spin state). High-pressure experiments indicate that iron occurs in both the ferrous and ferric state in the lower mantle, and that the effect of spin transitions on transport properties can be profound (Fig. 9.5).

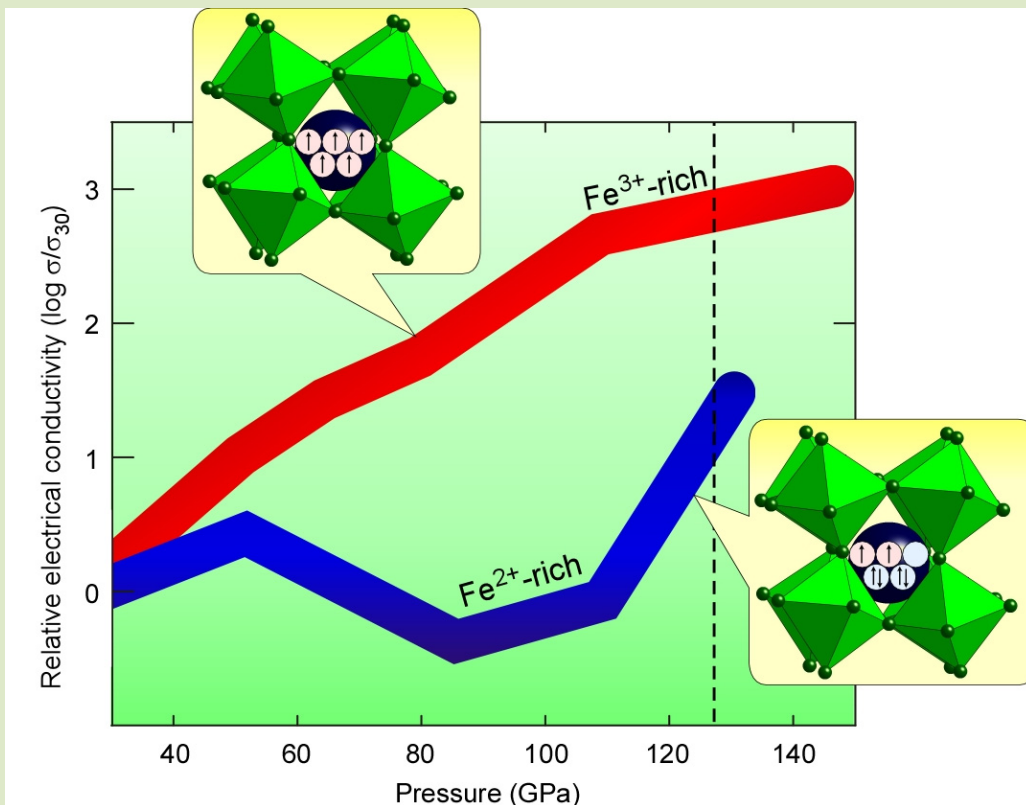
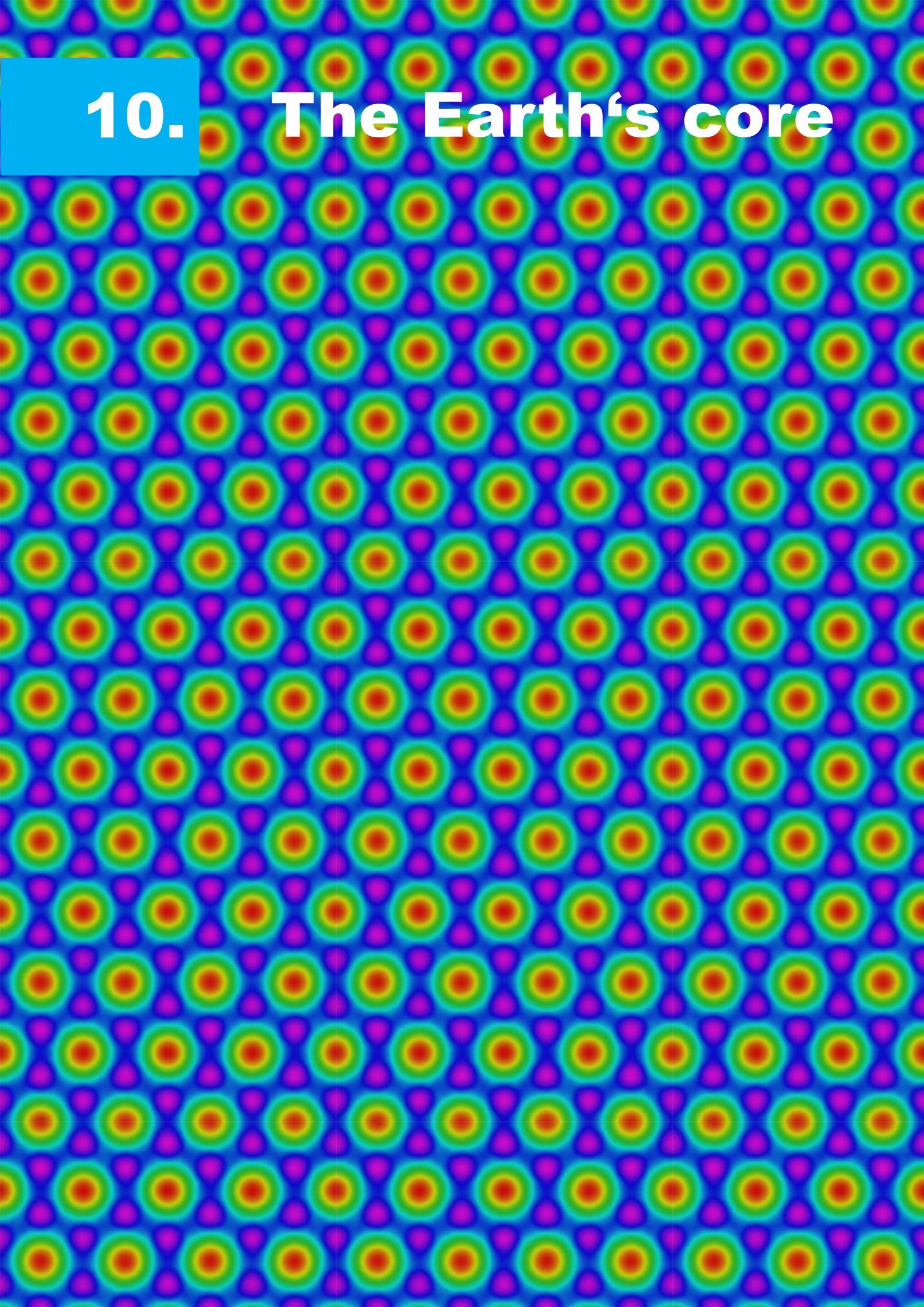


Fig. 9.5: Increasing pressure causes a profound drop in electrical conductivity of bridgmanite containing mostly ferrous iron (blue line), while there is no drop in electrical conductivity for perovskite containing mostly ferric iron (red line). The difference is attributed to a spin transition of ferrous iron that causes partial pairing of electrons.

**10.**

# **The Earth's core**



The core at the centre of the Earth covers about half the radius of our planet and is remote in the sense that we can never expect to get there, nor even retrieve a sample from it. Nevertheless, our knowledge about the core is substantial and continues to grow through remote sensing, geodynamic models and experimental work at high pressure. Despite its remoteness, the core plays an important role for life on Earth, as it is the region where the magnetic field is created that shields us from much of the dangerous charged particles that the sun emits into space.

Based on seismology, we have known for almost half a century that the core is divided into a liquid outer and a solid inner core, and we have good estimates of the seismic wave propagation velocities and density throughout the core. Currents created in the outer core through the motion (convection) of a metallic liquid have been identified as the source of the Earth's magnetic field. Cosmochemical arguments derived from iron meteorites (Fig. 10.1) and the abundance of chemical elements in the sun and therefore the solar system strongly suggest that the core is composed of iron, or

rather an iron-nickel alloy with 5-15 % of nickel. Light elements must also be abundant in the core, as we will see in the next paragraph.

In order to determine relevant physical properties of iron and iron alloys, experiments must be performed at the pressure and temperature of the core. There, pressures range from 136 to 365 GPa at the core-mantle boundary and the Earth's centre, respectively, and temperatures are in excess of 4000 K. To achieve such conditions in the laboratory is difficult even for laser-heated

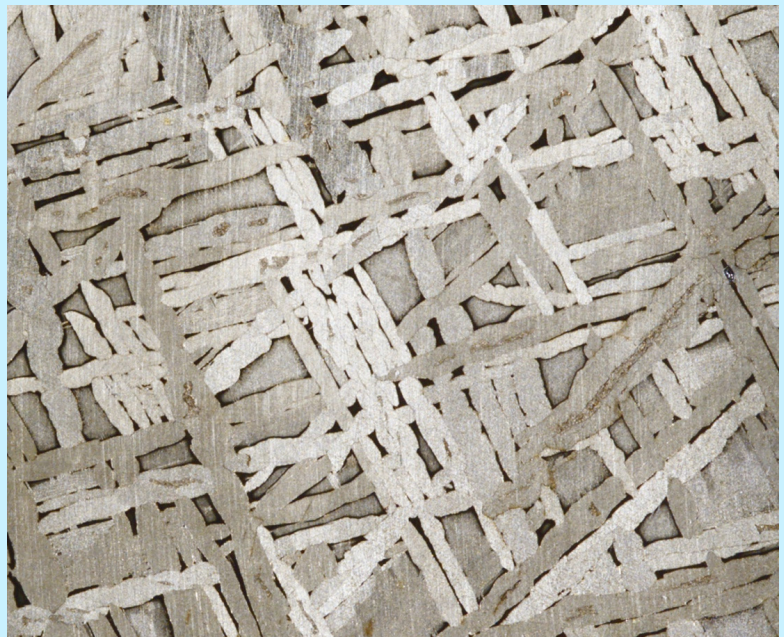


*Fig. 10.1: Polished section of an iron meteorite, a fragment of the core of a smaller planetary body in the asteroid belt. The typical pattern (Widmanstätten pattern) results from the exsolution of Ni-rich taenite and Ni-poor kamacite upon slow cooling.*

diamond anvil cells (see Chapter 2), and to this date shock wave experiments are the most important tool to determine physical properties of core material at the relevant conditions. Measurements of density and acoustic wave velocities in shock experiments, for example, have led to the understanding that the presence of light elements in addition to Fe is required to match the density in the Earth's core, with less light elements present in the inner core than in its outer liquid part. Based on cosmochemical arguments, H, C, O, Mg, Si, and S have been proposed as candidates. Due to a lack of relevant data at core conditions and the inherent non-uniqueness of their influence on density and seismic wave propagation velocities, geophysics alone may not be able to establish the light element composition of the Earth's core. Geochemical constraints on the partitioning of the candidate light elements between silicates and iron during core formation at pressures of the magma ocean that governed the early Earth (see Chapter 4), as well as between liquid iron and the solid phase of iron in the outer and inner core, respectively, may be of great help.

Representing a liquid-solid phase transition, the boundary between the outer and the inner core provides a fixed point on the geotherm, *i.e.*, the temperature in the core. If one knew the melting (or

rather liquidus) temperature of the outer core liquid at the pressure of the inner core boundary (*ca.* 330 GPa), this would establish a core temperature. Different experiments, which rely on the extrapolation of results to the pressure of the inner core boundary, and computations of the melting point, however, do not yield consistent results even for pure iron. Further technical advances in order to create such high pressures and temperatures in a stable fashion as well as experimental techniques to unequivocally detect melting are therefore of critical importance. In the outer core, magnetic field generation depends on the efficiency of the dynamo process that is balanced by a competition between dissipation (diffusion) of the magnetic field and the creation of new currents. This balance is critically influenced by the electrical conductivity of liquid iron-alloys, a property that is experimentally inaccessible at high pressure to this day. Here, molecular dynamics simulations at conditions of the Earth's core, first performed at Bayerisches Geoinstitut, and subsequently confirmed in other computational studies and supported by experimental studies on solid iron at much lower pressure, have revealed that the electrical conductivity of liquid Fe at core pressure and temperature is significantly larger than previously assumed, making magnetic field creation more efficient.

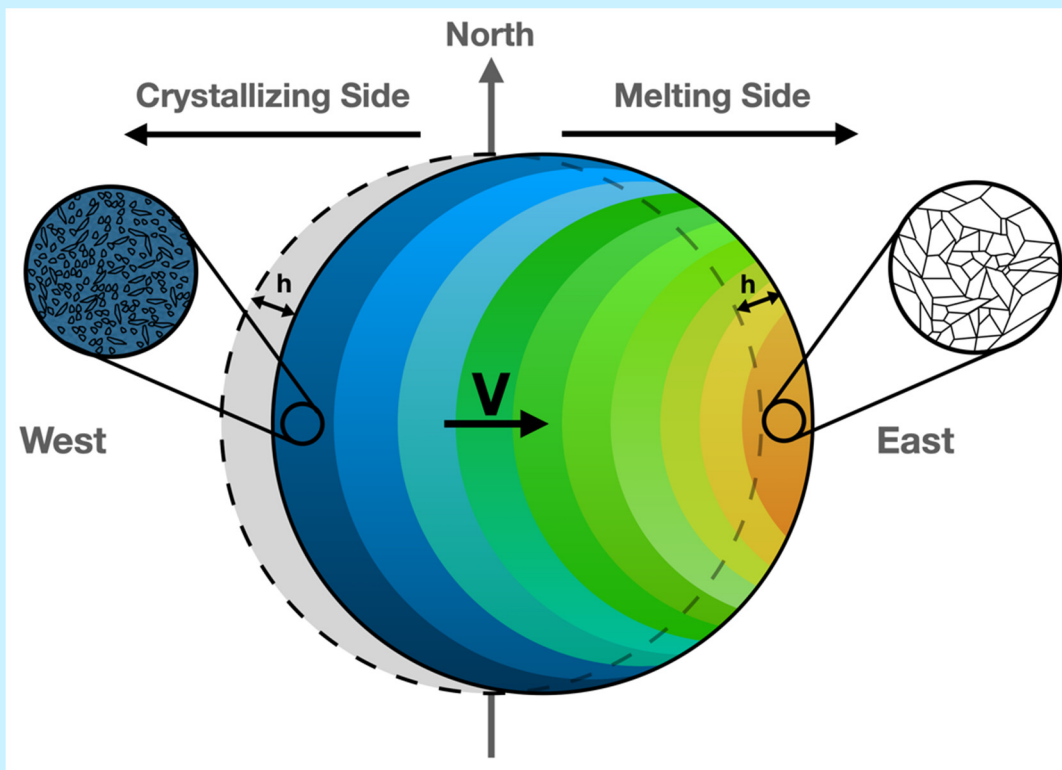


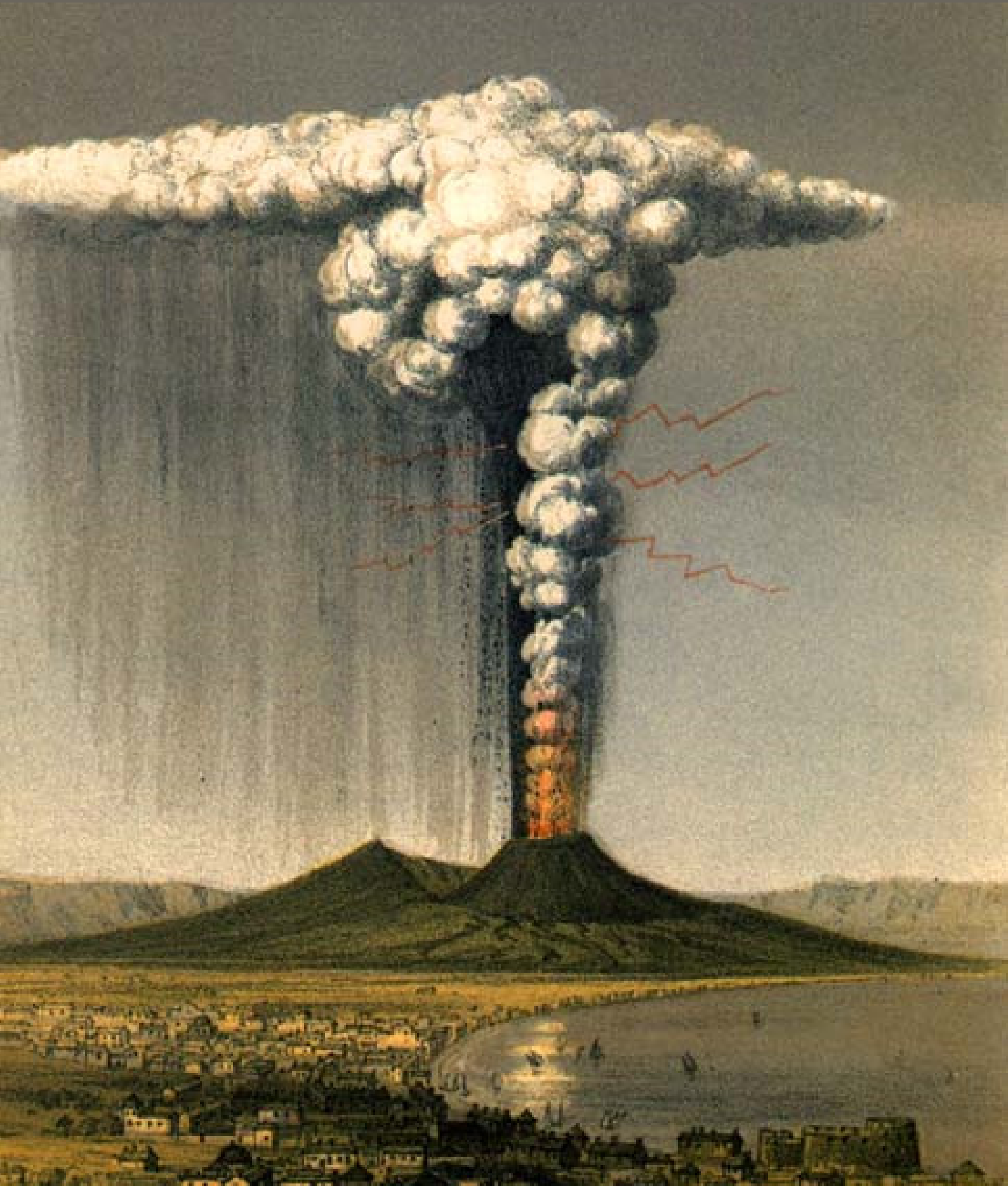
*Fig. 10.2: Schematic cross section through the inner core, illustrating a recent growth model. The Western hemisphere is assumed colder and consequently crystallisation of the inner core occurs there. The centre of mass is then shifted to the East to restore gravitational equilibrium, and partly remelts there in a hotter environment. The main consequences are an age increase of inner core material from W to E and associated grain growth.*

The solid inner core has long been thought to be an inert and featureless body at the centre of the Earth. The discovery that this body is seismically strongly anisotropic and has small scale heterogeneity has been a puzzle to scientists studying the dynamic evolution, especially growth, of the inner core. Many ideas have emerged that try to account for the seismological signature of the inner core, including a model in which the inner core grows in the Western hemisphere only, while it remelts in the Eastern hemisphere (Fig. 10.2). In

order for such a model to be predictive, knowledge about the elastic properties of iron and its crystalline structure at the conditions of the inner core is required, another challenge to mineral physics. Similar to conductivity in the Earth's outer core, computational studies provide important constraints here. For example, in a recent molecular dynamics study, mineral scientists have been able to explain why the inner core – as a solid body – has an extremely low rigidity, *i.e.*, a low elastic shear modulus.

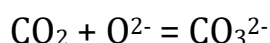
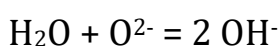
# 11.

# Volcanism



## Understanding and forecasting volcanic eruptions

Volcanic eruptions can be very different in character, ranging from a continuous outpouring of magma to violent explosions that inject particles into the stratosphere, as in the Mt. Vesuvius eruption shown on the previous page. A key parameter that controls eruption behaviour is the content and speciation of volatiles in the melt. Ultimately, the exsolution of dissolved gases, mostly H<sub>2</sub>O and CO<sub>2</sub>, is what powers any explosive eruption. Moreover, the dissolution of volatiles changes the physical properties of the magma; already a few wt. % of H<sub>2</sub>O can reduce melt viscosities by orders of magnitude. With modern methods, most volcanic eruptions can be well predicted and understanding the physical processes of volatile exsolution is an essential backbone of prediction. At Bayerisches Geoinstitut, extensive research has therefore been carried out on the dissolution of volatiles in magmas and on their effect on magma properties. The behaviour of water and CO<sub>2</sub> in melts is complicated by the fact that different species may coexist in the melt, according to the reactions



To determine the equilibria between molecular H<sub>2</sub>O, CO<sub>2</sub>, OH<sup>-</sup> and CO<sub>3</sub><sup>2-</sup> in the melt, Bayerisches Geoinstitut scientists pioneered the application of infrared spectroscopy in externally heated diamond cells. These experiments showed that the speciation of volatiles in melt at magmatic conditions is quite different from that observed in quenched glasses. Another recent development at Bayerisches Geoinstitut is a cell with moissanite (SiC) anvils, which allows the direct observation of the nucleation and growth of gas bubbles in a magma (Fig. 11.1). The observations made with this cell allow a better understanding of the processes driving explosive volcanic eruptions. They show, for example, that spontaneous

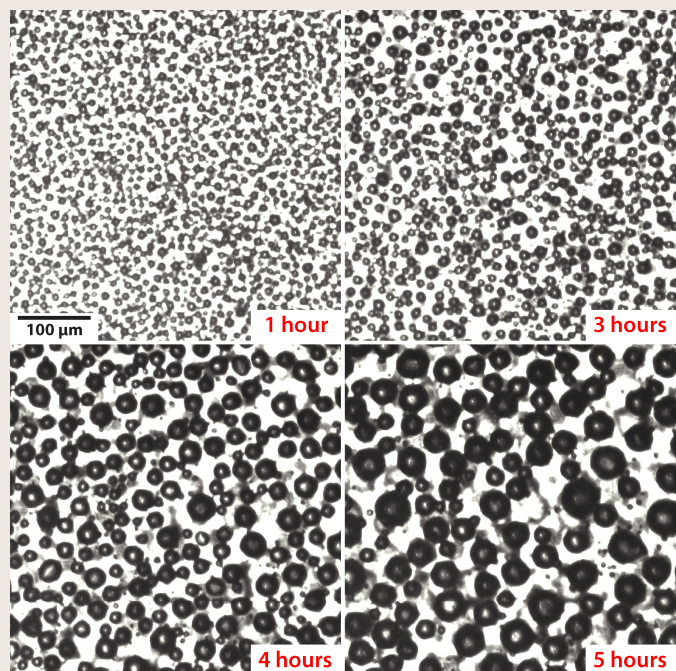


Fig. 11.1: Exsolution and growth of gas bubbles in a rhyodacite melt near 1100 °C as seen in a moissanite anvil cell.

bubble coalescence is a major mechanism by which gas bubbles grow in a melt.

### Volcanoes and climate

In the year of 1816, summer had disappeared from central Europe; in some areas, snow fell in July. Lord Byron wrote in June 1816:

*The bright sun was extinguish'd and the stars  
did wander darkling in the eternal space  
rayless, and pathless, and the icy earth  
swung blind and blackening in the  
moonless air*

At the same time, unusual discolorations of the sky were observed, particularly at sunrise and at sunset. Some paintings by William Turner with completely yellow skies probably give an impression of the appearance of the atmosphere at that time. The cause of these effects was the eruption of Tambora on Sumatra in 1815, which released  $50 \text{ km}^3$  of magma, ten times more than the Mt. Pinatubo eruption of 1991. Such explosive eruptions inject enormous quantities of  $\text{SO}_2$  into the stratosphere, where it is photochemically oxidised to  $\text{H}_2\text{SO}_4$  aerosols (Fig. 11.2). The aerosols may remain in the stratosphere for years and by backscattering sunlight, they cool Earth's surface. In or-



*Fig. 11.2: Space Shuttle images of the atmosphere at sunset, before (top) and one month after (bottom) the 1991 Mt. Pinatubo eruption. Two aerosol layers can be seen in the picture taken after the eruption.*

der to predict the impact of explosive eruptions on climate, the behaviour of sulphur during an eruption therefore has to be understood. Research at Bayerisches Geoinstitut has shown that sulphur partitions very strongly into an aqueous fluid phase in equilibrium with a silicate melt, such that a very small fraction of a gas phase may extract most of the sulphur from a magma chamber. This is likely the cause for the so-called "sulphur excesses" observed for major

explosive eruptions. The "sulphur excess" refers to the observation that often much more sulphur is released by an eruption than could have degassed from the erupted magma alone. Recent work in Bayreuth has also shown that adsorption processes on ash surfaces occurring inside the eruption plume may under some circumstances reduce the amount of SO<sub>2</sub> and HCl reaching the stratosphere.

### Reading volcanic rocks

Volcanic rocks preserve important information on magmatic processes that occurred recently or in deep geologic time. Mineral assemblages and the compositions of coexisting phases constrain the pressure and temperature conditions of magma generation, storage, and crystallisation. The textures of rocks – the sizes, shapes, and relative arrangement of crystals – could in principle

yield complementary information on the rate of volcanic processes. However, attempts to use CSD (crystal size distribution) theory to extract the timescales of magmatic processes from textures so far had only limited success. This is mostly due to the inability to observe the crystallisation of magmas and the corresponding texture evolution *in situ*. The high-temperature moissanite cell developed in Bayreuth now allows such experiments (Fig. 11.3). The experimental data show that the nucleation of crystals is limited to short events, followed by long periods of crystal growth. The growth rate of olivine crystals in basalt melt is not uniform; rather, the growth rate increases with crystal size. This effect of proportionate growth was before only observed in low-temperature analogue systems. Taken together, the experimental observations show that the current interpretations of crystal size distributions need to be revised.

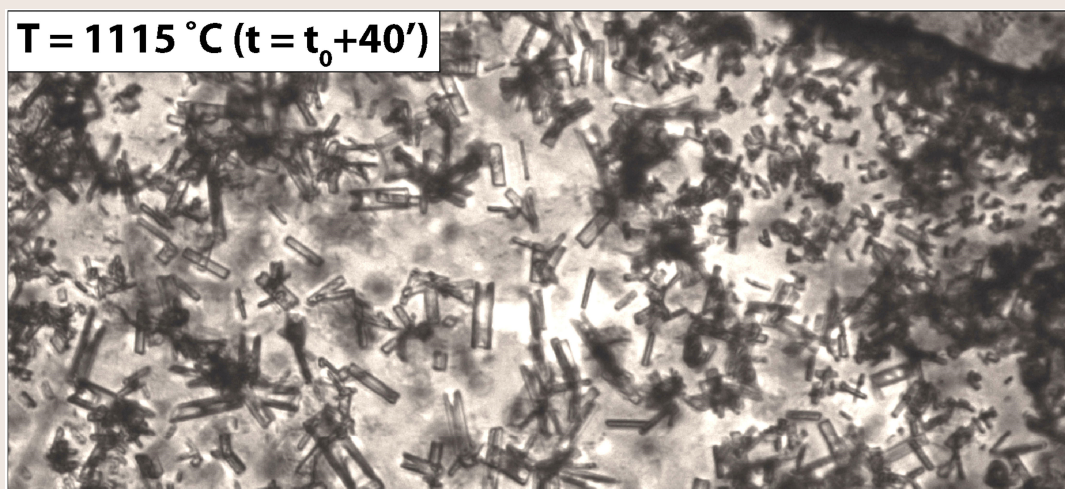
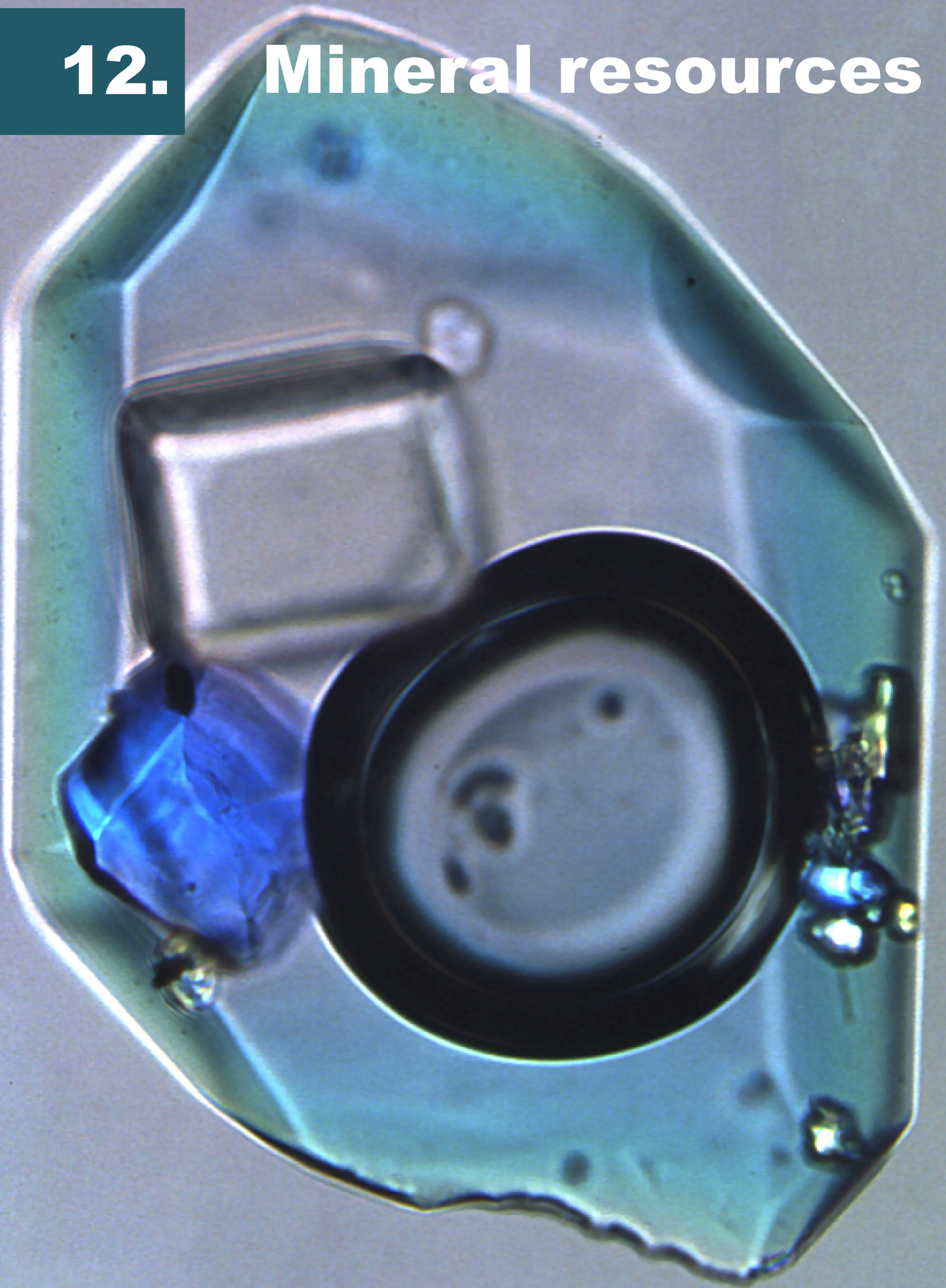


Fig. 11.3: Olivine crystallisation from a basaltic melt, as seen in a moissanite cell.  $t_0$  is the time when the liquidus was reached. Width about 500  $\mu\text{m}$ .

**12.**

# Mineral resources



Ore deposits have played a key role in the evolution of humankind since its earliest history. Strategic and economically important metals such as Cu, Au, Mo, Sn, W, U, Nb, Ta and rare earths occur in deposits that are genetically related to magmatic intrusions. These deposits have been formed by hot, hydrothermal solutions. Information on the metal content of magmatic-hydrothermal fluids and the mechanisms of metal

complexing in these fluids is thus of fundamental importance for understanding the formation of such deposits and to develop models that allow the finding of new deposits. Modern microanalytical techniques, such as laser-ablation ICP-MS, which may detect elements at the ppm level in volumes of less than  $1000 \mu\text{m}^3$  (e.g.,  $20 \times 10 \times 5 \mu\text{m}^3$ ), now allow metal concentrations to be determined in tiny fluid inclusions that were

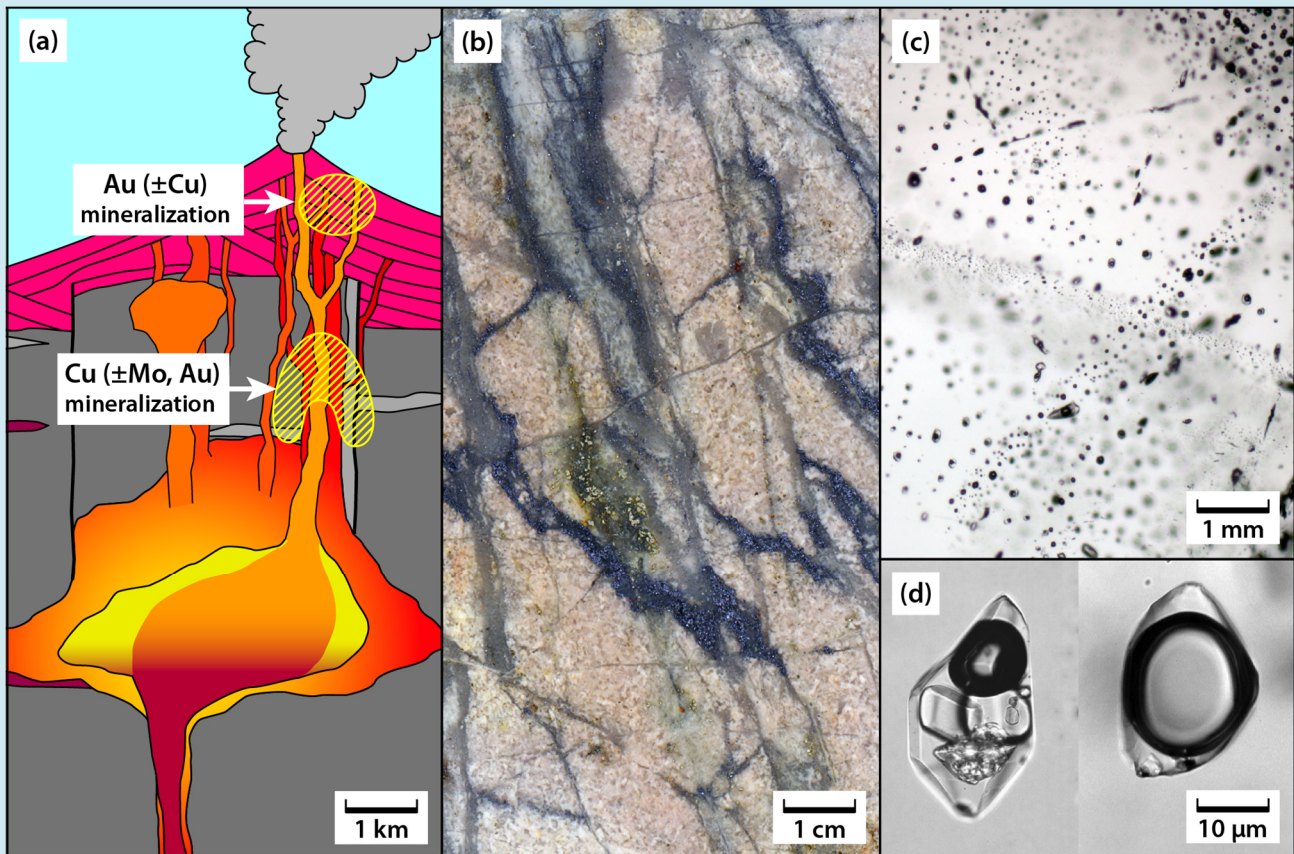


Fig. 12.1: (a) Schematic cross section through a Cu- and Au-mineralised magma system. Porphyry-type Cu ( $\pm$ Mo, Au) mineralisation occurs at 3-4 km depth beneath the stratovolcano; epithermal Au ( $\pm$ Cu) mineralisation occurs at shallow levels. (b) Porphyry-type ore with quartz veins (grey), MoS<sub>2</sub> (dark blue) and CuFeS<sub>2</sub> (yellow). (c) transmitted-light photomicrograph of a polished thick section of a quartz vein, showing numerous fluid inclusions (dark spots) on healed fractures. (d) close-up view of two fluid inclusions that are representative of a chloride-rich brine (left) and a low-density vapour phase (right). Both inclusions formed millions of years ago and provide information regarding the type and metal content of the mineralising fluids.

## Mineral resources

trapped in quartz millions of years ago during the formation of the ore deposits (Fig. 12.1).

At the pressure and temperature conditions of magmatic-hydrothermal ore formation (typically 300-700 °C and 10-100 MPa), saline fluids were boiling, i.e., they consisted of a salt-rich brine phase coexisting with a low-density vapour phase. If trapped within cracks of growing quartz crystals, the two fluid phases gave rise to two contrasting types of fluid inclusions: salt-rich brine inclusions and low-density vapour inclusions. Traditionally, brines were considered as the dominant fluid medium for

ore formation, because many metals form stable complexes with chlorine and thus should prefer the brine phase over the vapour phase. However, analyses on natural pairs of coexisting vapour and brine inclusions returned the unexpected result that copper commonly is enriched in the vapour phase, particularly if the vapour was sulphur rich. This has led to the hypothesis that copper was complexed by reduced sulphur (as has been demonstrated for Au) and that vapour-type fluids played a much more important role in the Cu-mineralisation process than previously thought.

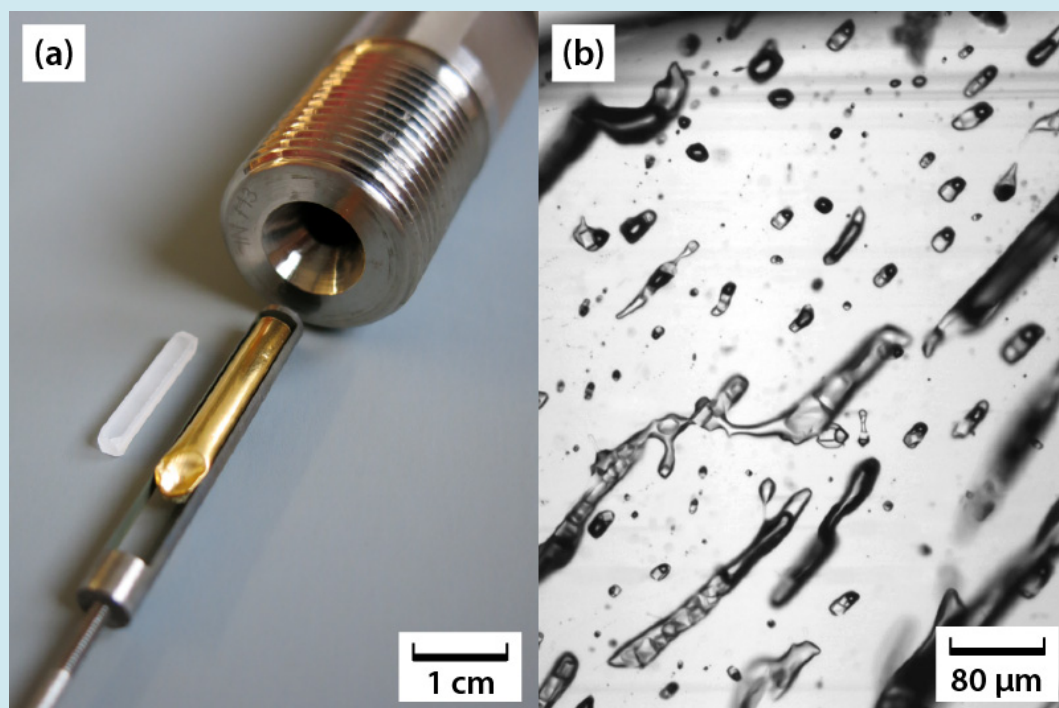
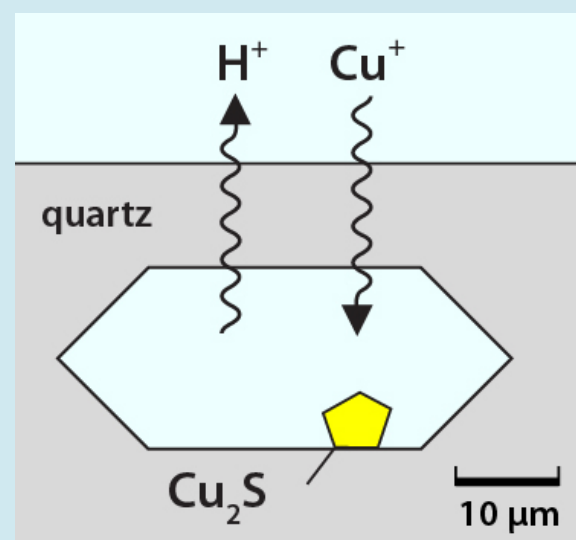


Fig. 12.2: (a) Cold-seal pressure vessel with quartz piece and gold capsule. (b) Synthetic fluid inclusions in quartz, produced at 800 °C and 1.5 kbar. The coexistence of vapour-rich inclusions with salt-rich inclusions demonstrates that the fluid was two-phase (boiling) during the experiment.

Several experimental geochemistry groups worldwide thus set off to study the behaviour of Cu in two-phase fluids by means of synthetic fluid inclusions (Fig. 12.2). Strangely enough, however, no one was able to reproduce the high vapour/brine partition coefficients recorded in the natural fluid inclusions. After numerous failed attempts the research group at Bayerisches Geoinstitut was finally able to demonstrate by re-equilibration experiments that the record of natural fluid inclusions is corrupted, with the vapour inclusions having gained Cu after their formation (Fig. 12.3). Cu-diffusion was driven by the cooling of magmatic-hydrothermal fluids, during which the fluid pH typically evolves from strongly acidic to  $\pm$  neutral. Because small, single-charged ions like  $H^+$  can easily diffuse through the quartz structure, protons from the early, acidic fluid trapped within the fluid inclusions diffuse into the younger, less acidic fluid outside the quartz crystal. In order to maintain the charge balance,  $Cu^+$ -ions (and to a lesser degree also  $Ag^+$ -ions) diffuse from the surrounding fluid into the fluid inclusion and combine there with sulphur to form solid copper sulphide. This process continues until nearly all of the sulphur within the fluid inclusion is used up. Since the vapour phase is more acidic and usually contains more sulphur than

the brine phase, vapour inclusions gain more Cu.

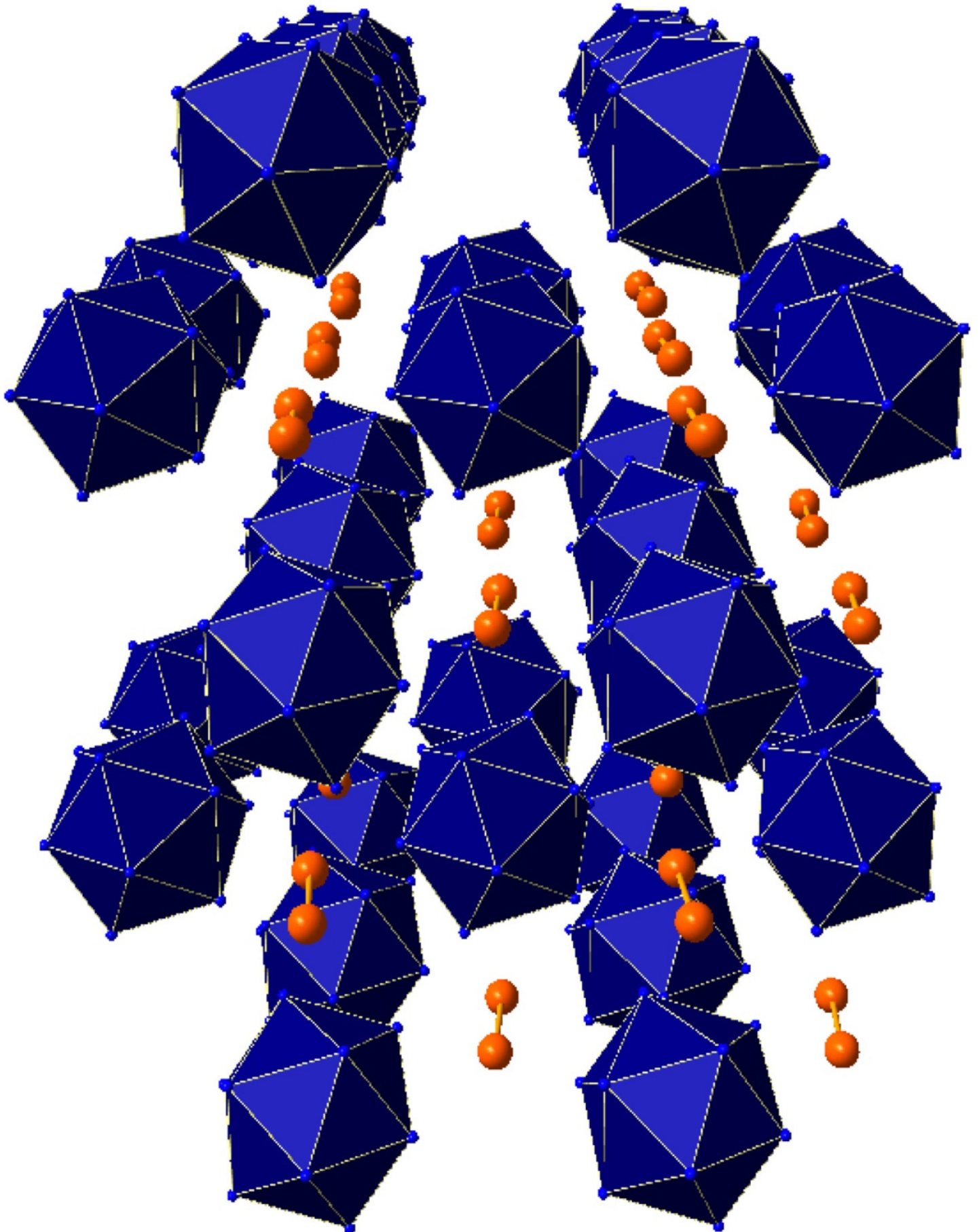
The results of this study help to re-define models of porphyry-Cu ore formation and their link to overlying epithermal Au deposits. Sulphur-bearing vapour physically separates from the heavy brine at depth and preferentially transports Au, but not Cu from the porphyry environment to the overlying epithermal environment. This is the main reason why Cu and Au are enriched in two different types of deposits originating from the same magmatic-hydrothermal system (see Fig. 12.1a).



*Fig. 12.3: Model explaining the diffusive uptake of Cu in fluid inclusions during equilibration in a fluid with increased pH: protons diffuse from the acidic fluid within the fluid inclusion to the less acidic outer fluid. In return, Cu ions diffuse into the fluid inclusion and combine with sulphur to form copper sulphide. This process continues until nearly all sulphur within the inclusion is bound in  $Cu_2S$ .*

**13.**

# **Technological applications**



The study of Earth materials teaches us that crystal structures and properties change with pressure and temperature, and that these parameters are therefore useful tools for synthesising novel materials. Pressure allows the precise tuning of a single fundamental parameter, interatomic distance, which in turn controls the electronic structure and therefore material properties.

The only material that is currently produced on an industrial scale by high-pressure synthesis is diamond. Indeed, most of the diamond that is currently used for example in the drilling equipment of oil industry is synthetic. Producing materials with a hardness similar to or even higher than diamond is one of the main directions of applied high-pressure research. Although hardness is a macroscopic phenomenon, the crystal structure, which describes bonds lengths and bond angles is the decisive factor for the strength of any material. Diamonds are generally considered to be the hardest known material due to the directed covalent  $sp^3$  bonds between carbon atoms that give rise to a very rigid structure. In contrast, graphite, the other main polymorph of carbon, contains three strong short bonds within the sheets and a very long bond between sheets. The easy shear between graphite sheets makes it an ideal material for old-fashioned pencils and high-tech lubricants; whereas the hardness of diamond makes it an exceptional abrasive for many applications.

Unfortunately, diamonds cannot be used to machine ferrous metals, presumably because a metal carbide is formed under the high-temperature conditions encountered during the machining process, or because iron catalyses the transformation of diamond back to graphite. Hence there is a great need for thermally stable materials with hardness approaching (or even greater than) that of diamond for use in the machining of ferrous metals.

So far it has been hard to imagine that the outstanding properties of diamond could be significantly improved. However, studies of nanomaterials have shown that their properties (*e.g.*, hardness and thermal stability) may exceed those of bulk materials. In particular, it was suggested that carbon clusters with a diamond-like structure ("nanodiamond") with diameters less than about 5 nm (1 nm = 1 billionth of a metre) may actually be more stable than graphite-like clusters of the same size. At Bayerisches Geoinstitut, samples of nanocrystalline cubic diamond with crystallite sizes of 5-12 nm were synthesised. We found that the hardness of the new material exceeded that of single crystal diamond. As shown in Figure 13.1, these materials scratch the hardest face of diamond and are therefore harder – a revival of the Mohs scale of hardness test. This nanocrystalline diamond is even thermally and kinetically more stable than conventional diamonds – its oxidation in air or transformation to graphite

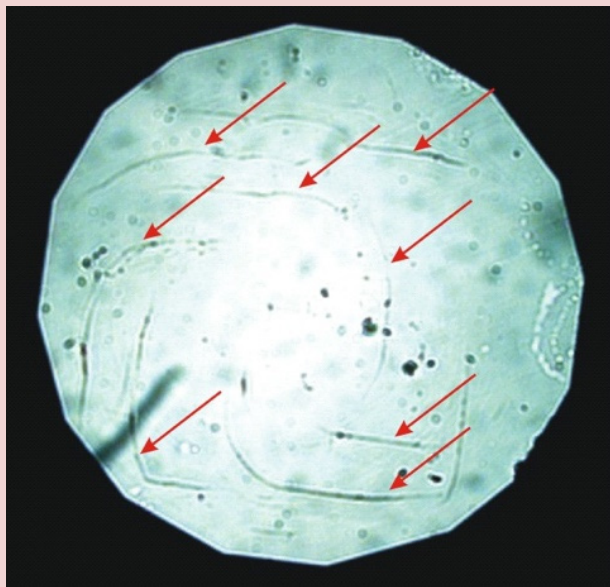


Fig. 13.1: Photograph of the "hardest" (111) face of natural diamond scratched by synthetic nanodiamond (arrows). The edge of the picture is  $350\ \mu\text{m}$  across.

are slower at high temperature than for coarse-grained diamond.

Research on superhard materials is not exclusively confined to diamond-like structures. Hard and superhard materials are also encountered among oxides, nitrides and carbides, and some of these are important from both a geophysical and a technological perspective. The results of studies on high  $P$ - $T$  polymorphs of silica, titania, and silicon nitride have shown that stishovite (rutile-type  $\text{SiO}_2$ ),  $\alpha$ - $\text{PbO}_2$ -like silica, cotunnite-type  $\text{TiO}_2$ , and cubic  $\text{Si}_3\text{N}_4$  are all harder than  $\text{Al}_2\text{O}_3$  (recall that corundum has a hardness of 9 on the Mohs scale), which make them among the hardest known polycrystalline materials.

Methodologically, hardness is a difficult parameter to assess in newly synthesised materials, since sufficiently large quantities of material are needed, and hardness (generally measured as Vickers hardness using a diamond indenter) is not defined when the hardness of a material exceeds that of diamond. On the other hand, the isothermal bulk modulus  $K_T$  of a material can be easily measured with high precision, and is closely related to hardness as illustrated in Figure 13.2. Through the combination of various synthesis methods (electrically heated diamond cell for extreme pressures, multianvil presses for larger volumes) with advanced methods of *in situ* or *ex situ* characterisation (for example using X-rays, vibrational or Mössbauer spectroscopy), we have the potential to discover new materials that have innovative technical applications.

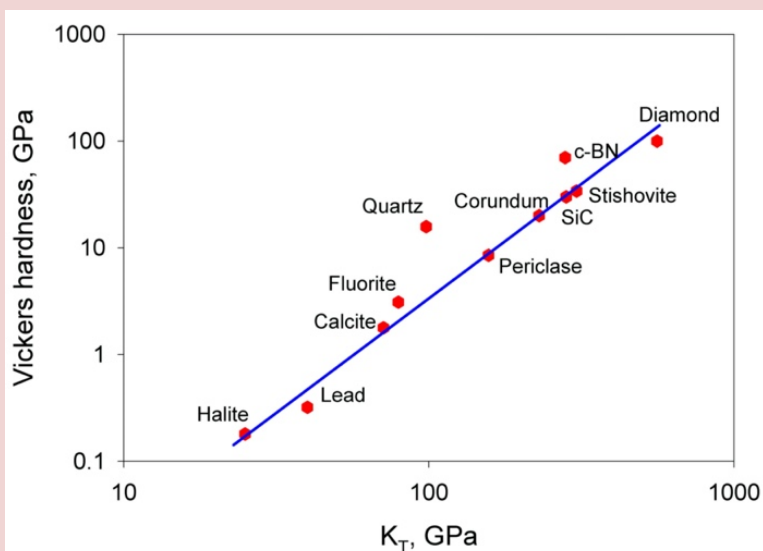
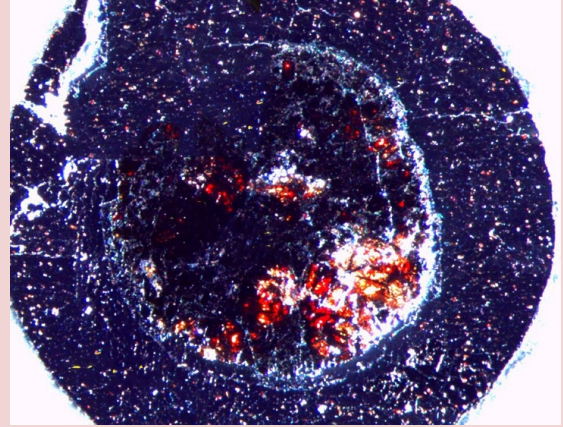


Fig. 13.2: Diagram showing the relationship between Vickers hardness  $H$  and the isothermal bulk modulus  $K_T$  for a number of materials. Note the logarithmic scales.

Elemental boron was until recently a material with an enigmatic phase diagram. In the course of studies on the high-pressure/high-temperature behaviour of boron, scientists at Bayerisches Geoinstitut synthesised some new polymorphs, developed a unique methodology for growing single crystals of different phases (Fig. 13.3), and revealed their structural details. All boron allotropes contain covalently bonded  $B_{12}$  icosahedra. Due to the strong chemical bonding between atoms, they show exceptional hardness (45 to 60 GPa, among elements second after diamond), and a unique combination of unusual properties – they are wide-bandgap semiconductors, optically transparent and thermally stable (above 1000 K in air). The possibility to grow single crystals of boron phases at relatively low pressures opens perspectives for using these materials in electronics and optics.

Manganites,  $MeMnO_3$  (where Me is a metal or combination of metals) are one of the most interesting sub-classes of perovskites revealing numerous novel phenomena, including colossal magneto-resistance near the Curie temperature, dense granular magneto-resistance, and optically-induced magnetic phase transitions. In all manganites, the Mn ions exclusively occupy octahedrally-coordinated B-sites in the crystal structure. Moreover, so far there were no known  $Me_2O_3$  (where Me is metal, including Mn) oxides with the



*Fig. 13.3: Platinum capsule from a multi-anvil experiment containing red crystals of  $\alpha$ -boron grown at high pressure. Diameter is about 1 mm.*

perovskite structure. By high-pressure/high-temperature synthesis, we obtained perovskite-like manganese oxide. The structural, mechanical, optical, and magnetic properties of perovskite-type  $Mn_2O_3$  suggest that there is no charge separation between structural manganese positions. This new oxide semiconductor has a narrow and direct band gap of 0.45 eV and a high Vickers hardness of 15 GPa. All known materials with similar electronic band structures (*e.g.*, InSb, PbTe, PbSe, PbS, and InAs) play crucial roles in the semiconductor industry. Furthermore, this material may reversibly 'switch' the electrical conduction type under applied load. The perovskite-type  $Mn_2O_3$  consists of non-toxic, abundant and inexpensive elements, it is much more incompressible and stronger than the above-mentioned semiconductors, and a unique combination of its electronic and mechanical properties makes it particularly promising for applications.

14.

# About Geoinstitut



**Mission:** Bayerisches Geoinstitut is a central research facility at the University of Bayreuth. The institute was founded in 1986 with the goal to investigate processes in the Earth's interior through experimental studies at high pressures and high temperatures.

**Staffing and structure:** The institute currently has five professorships, three in the fields of experimental geosciences, one for geodynamic modelling, and one for cosmochemistry. Moreover, there are ten senior scientific staff positions and a technical and administrative staff of 16. Together with numerous, mostly externally funded postdocs, Ph.D. students and long-term visitors, there are usually close to 100 people working at the institute. The professors are also *ad personam* members of the Faculty for Biology, Chemistry and Geosciences. The institute is headed by an acting director. The absence of a formal group structure and an "open lab door" philosophy helps to overcome barriers between disciplines. The "Beirat für Geowissenschaftliche Hochdruckforschung" of the Bavarian Academy of Sciences in Munich acts as an advisory body.

**National and international collaboration:** Through the institute's visiting scientists' programme, EU-funded exchange programmes for junior and

senior scientists, fellowship and award programmes of the Alexander von Humboldt Foundation, *etc.*, the institute offers a truly international, challenging, and friendly atmosphere. This spirit, combined with the expertise of the staff, the unique experimental equipment and the excellent technical support staff, makes the institute attractive for Ph.D. students, postdoctoral fellows and senior scientists from all over the world. Bayerisches Geoinstitut has close ties to several research institutions abroad, including Tohoku University and the Geodynamics Research Center at Ehime University in Japan (Fig. 14.1). The institute operates instruments and laboratories at various large-scale facilities, including the SAPHiR instrument for high-pressure neutron diffraction and radiography at the FRM II neutron source in Garching.

**Teaching:** A master course in "Experimental Geosciences" integrates students into research projects already starting from the first semester. Once a year, a laboratory course on "High pressure experimental techniques and applications to the Earth's interior" is held in Bayreuth, with a strong international participation from graduate and postgraduate students. A large group of international Ph.D. students at the institute is central for most research projects. The professors at the institute

**Equipment:** Major equipment includes

### I. High-pressure apparatus

- 15 MN/1500 tonne Kawai-type multianvil high-pressure apparatus (40 GPa, 2000 K)
- 6 x 8 MN/6x800 tonne independently acting-anvil press (25 GPa, 3000 K)
- 50 MN/5000 tonne multianvil press (25 GPa, 3000 K)
- 12 MN/1200 tonne multianvil press (25 GPa, 3000 K)
- 10 MN/1000 tonne multianvil press (25 GPa, 3000 K)
- 5 MN/500 tonne multianvil press (20 GPa, 3000 K)
- 5 MN/500 tonne press with a deformation DIA apparatus
- 5 piston-cylinder presses (4 GPa, 2100 K)
- Cold-seal vessels (700 MPa, 1100 K, H<sub>2</sub>O), TZM vessels (300 MPa, 1400 K, Ar), Rapid-quench cold-seal vessels (400 MPa, 1200 K, H<sub>2</sub>O)
- Internally-heated autoclave (1 GPa, 1600 K)
- High-pressure gas loading apparatus for DAC

### II. Structural and chemical analysis

- 1 X-ray powder micro-diffractometer
- 1 X-ray powder diffractometer with furnace and cryostat
- 2 automated single-crystal X-ray diffractometers
- High-brilliance X-ray system
- Single crystal X-ray diffraction with super-bright source
- 1 Mössbauer spectrometer (1.5 - 1300 K)
- 3 Mössbauer microspectrometers
- 2 FTIR spectrometers with IR microscope
- FEG transmission electron microscope (TEM), 200 kV analytical, with EDS
- FEG scanning TEM, 80-200 kV analytical, with 4-SDDs EDS and post-column energy filter (EFTEM/EELS)
- FEG scanning electron microscope (SEM) with BSE detector, EDS, EBSD and CL
- Dual beam device, focused ion beam (FIB) and FEG SEM. In situ easy-lift manipulator, STEM, EDS and EBSD detectors, and beam deceleration option
- 3 Micro-Raman spectrometers with ultraviolet and visible lasers
- Tandem-multipass Fabry-Perot interferometer for Brillouin scattering spectroscopy
- JEOL JXA-8200 electron microprobe; fully-automated with 14 crystals, 5 spectrometer configuration, EDX, capability for light elements
- 193 nm Excimer Laser-Ablation ICP-MS
- Water content determination by Karl-Fischer titration
- GC/MS-MS for organic analyses
- Confocal 3D surface measurement system
- 1.4 Tesla sweepable ESR magnet
- Solid state 300 MHz NMR spectrometer

### III. *In situ* determination of properties

Diamond anvil cells for powder and single crystal X-ray diffraction, Mössbauer, IR, Raman, optical spectroscopy, NMR spectroscopy, electrical resistivity measurements over 200 GPa

Facility for *in situ* hydrothermal studies in DAC

Externally heated DACs for *in situ* studies at pressures to 100 GPa and 1200 K

1-atm furnaces to 1950 K, gas mixing to 1600 K, zirconia  $fO_2$  probes

1-atm high-temperature creep apparatus

Gigahertz ultrasonic interferometer with interface to resistance-heated diamond-anvil cells

Freezing-heating stage for fluid inclusion studies

Impedance/gain-phase analyser for electrical conductivity studies

Apparatus for *in situ* measurements of thermal diffusivity at high P and T

Laser-heating facility for DAC

Portable pulsed laser heating system for DAC

also provide the basic training in geology for students of geography and environmental science at the university, as well as advanced courses, *e.g.*, for physics or chemistry students.

**Funding:** Bayerisches Geoinstitut receives generous funding from the State of Bavaria. Important complementary funds come from the European Union through various programmes (notably the ERC), the German Science Foundation (DFG), and Alexander von Humboldt Foundation. Many visitors bring their own funds in the form of stipends or awards from the Alexander von Humboldt Foundation, DAAD, EU, and national agencies abroad.

**Annual Report:** The institute issues a comprehensive Annual Report on its scientific activities once a year, giving summaries of recent projects, a list of publications by staff members, lectures held, conferences organised, visitors hosted, *etc.* These Annual Reports can also be viewed on the institute's web page ([www.bgi.uni-bayreuth.de](http://www.bgi.uni-bayreuth.de)).

**The Building:** Bayerisches Geoinstitut is based on the campus of the University of Bayreuth and occupies the major fraction of the "BGI" building, with four large laboratories (400 m<sup>2</sup>, multianvil, deformation, piston-cylinder, internally heated autoclaves), some 760 m<sup>2</sup> of additional lab space, 450 m<sup>2</sup> of office space, 280 m<sup>2</sup> of machine shops and 70 m<sup>2</sup> of infrastructure space (including seminar room, institute library, *etc.*).

## About Geoinstitut

Additional clean-lab facilities for isotope geochemistry and cosmochemistry are currently under construction. The institute also has access to the central machine shops, central library, computer centre, *etc.* of the University of Bayreuth.

The Geoinstitut is provided with well-equipped machine shops, electronic workshop and sample preparation laboratories.



Fig. 14.1: Participants of a joint Bayerisches Geoinstitut - Ehime University workshop in the park of the Eremitage in Bayreuth.



# Source of Figures, copyright information

We are grateful to the following copyright holders for permission to reproduce the figures in this brochure.

Fig. 1.1.....	© GEO 4/94, modified
Fig. 1.2.....	© R. Hollerbach, Köln. From Dreiser Weiher, Eifel Mountains, Germany, ..... Collection GeoMuseum, Universität Köln
Fig. 1.3.....	© J.J. Gurney, Cape Town
Fig. 1.4.....	© F. Heidelbach, Bayreuth
Fig. 1.5.....	© D. Zhao, et al. (1997), Ehime Universiy, Japan
Fig. 1.6.....	© F. Marton, Bayreuth
Fig. 1.7.....	© F. Seifert, Bayreuth
Fig. 2.1.....	© Bayerisches Geoinstitut, Bayreuth
Figs. 2.2, 2.3.....	© Bayerisches Geoinstitut, Bayreuth, S. Weber
Fig. 2.4.....	© Bayerisches Geoinstitut
Fig. 2.5, 9.4.....	© L. Dubrovinsky, Bayreuth
Fig. 2.6.....	© Min. Soc. Great Britain, see also <a href="http://www.minersoc.org">www.minersoc.org</a> , and courtesy ..... T. Arlt, Marly, Switzerland
Fig. 2.7.....	© G. Steinle-Neumann, Bayreuth
Fig. 3.1.....	© M. Giannini, Bayreuth
Fig. 3.2A.....	© A. El Goresy, Bayreuth
Fig. 3.2B.....	© M. Miyahara, Tohoku University, Sendai, Japan
Fig. 3.3.....	© S. Jacobsen, Northwestern University, Evanston
Fig. 3.4.....	© NASA/JPL/Space Science Institute
Fig. 4.1.....	© H. Terasaki, University of Osaka
Fig. 4.2.....	© NASA/JPL-Caltech
Fig. 4.3.....	© V. Laurenz, Bayreuth, and R. Fischer, Harvard Univ., Cambridge, USA
Fig. 4.4.....	© D. Rubie, Bayreuth
Fig 5.1, 5.2, 7.1.....	© D. Frost, Bayreuth
Fig. 6.1.....	© G. Bromiley, Bayreuth
Fig. 6.2.....	© H. Keppler, Bayreuth
Fig. 6.3.....	© (left) S. Demouchy, Bayreuth, (right) after Mierdel et al. 2007
Fig. 6.4.....	© S. Shcheka, Bayreuth
Fig. 6.5.....	© S. Shcheka, Bayreuth
Fig. 6.6.....	© E. Bali, Bayreuth
Fig. 7.1, 7.2.....	© D. Frost, Bayreuth
Fig. 8.1.....	© S. Shekhar, Bayreuth
Fig. 8.2.....	© F. Heidelbach, Bayreuth
Fig. 8.3.....	© N. Miyajima, Bayreuth
Fig. 9.1, 9.3, 9.5.....	© C. McCammon, Bayreuth
Fig. 9.2.....	© T. Chust, Bayreuth
Fig. 10.1.....	© A. Bischoff, F. Bartschat, Uni Münster
Fig. 10.2.....	© F. Trybel after Monnerau et al. (2010)
Fig. 11.1.....	© M. Massotta, Bayreuth
Fig. 11.2.....	© Images courtesy of NASA Scientific Visualization Studio
Fig. 11.3.....	© H. Ni, Bayreuth
Fig. 12.1a, b, c, 12.2.a, b, 12.3.....	© A. Audétat, Bayreuth
Fig. 13.1, 13.2.....	© N. Dubrovinskaia, Bayreuth
Fig. 13.3.....	© L. Dubrovinsky, Bayreuth
Fig. 14.1.....	© Bayerisches Geoinstitut

### Frontispieces:

Page 6.....	© F. Langenhorst, Bayreuth
Page 14.....	© S. Keyssner, Bayreuth
Page 20.....	© NASA, ESA, and The Hubble Heritage Team (STScI/AURA)
Page 24.....	© W.K. Hartmann, Tucson
Page 30.....	© N. Bolfan Casanova, CNRS, Clermont-Ferrand
Page 34.....	© R. Robinson, U.S. National Park Service
Page 42.....	© R. Myhill, Bayreuth
Page 46.....	© F. Heidelbach, Bayreuth
Page 50.....	© C. McCammon, Bayreuth
Page 54.....	© G. Steinle-Neumann, Bayreuth
Page 58.....	Historical drawing by George JP Scrope
Page 62.....	© A. Audétat, Bayreuth
Page 66.....	© L. Dubrovinsky, Bayreuth
Page 70.....	© Universität Bayreuth

Outside cover image: ..... © Sylvie Demouchy, Bayreuth  
Thin section of a mantle xenolith from Pali-Aike, Patagonia







